3-1-2015

Microgrid Optimal Scheduling Considering Impact of High Penetration Wind Generation

Abdulaziz Furreh Alanazi
University of Denver

MICROGRID OPTIMAL SCHEDULING CONSIDERING IMPACT OF HIGH PENETRATION WIND GENERATION

_____

A Thesis

Presented to

The Faculty of the Daniel Felix Ritchie School Of Engineering and Computer Science

University of Denver

_____

In Partial Fulfillment

of the Requirements for the Degree

Master of Science

_____

By

Abdulaziz Alanazi

March 2015

Advisor: Dr. Amin Khodaei

Author: Abdulaziz Alanazi
Title: MICROGRID OPTIMAL SCHEDULING CONSIDERING IMPACT OF HIGH PENETRATION WIND GENERATION
Advisor: Dr. Amin Khodaei
Degree Date: March 2015

Abstract

The objective of this thesis is to study the impact of high penetration wind energy in economic and reliable operation of microgrids. Wind power is variable, i.e., constantly changing, and nondispatchable, i.e., cannot be controlled by the microgrid controller. Thus an accurate forecasting of wind power is an essential task in order to study its impacts in microgrid operation. Two commonly used forecasting methods including Autoregressive Integrated Moving Average (ARIMA) and Artificial Neural Network (ANN) have been used in this thesis to improve the wind power forecasting. The forecasting error is calculated using a Mean Absolute Percentage Error (MAPE) and is improved using the ANN. The wind forecast is further used in the microgrid optimal scheduling problem. The microgrid optimal scheduling is performed by developing a viable model for security-constrained unit commitment (SCUC) based on mixed-integer linear programing (MILP) method. The proposed SCUC is solved for various wind penetration levels and the relationship between the total cost and the wind power penetration is found. In order to reduce microgrid power transfer fluctuations, an additional constraint is proposed and added to the SCUC formulation. The new constraint would control the time-based fluctuations. The impact of the constraint on microgrid SCUC results is tested and validated with numerical analysis. Finally, the applicability of proposed models is demonstrated through numerical simulations.

Acknowledgements

It has been one year now since started my work with wonderful advisor Dr. Amin Khodaei. It was an amazing experience in my life. He is a very supportive and helpful professor. A lot of challenges and obstacles were overcome by his guidance. Here it is the time to thank him for all of his assistance, which really helped me in my research and really improved my knowledge in my research area. Also, it is my honor to present my thesis in front of this grateful committee members, Dr. Mohammad Matin and Dr. Jun Zhang, and listen to their valuable observations, feedback and comments on my thesis. Moreover, I want to send my best regards to the external committee member, Dr. Caroline Li, for giving me some of her time and attending to my thesis defense. Last but not least, I should not forget to thank the Electrical and Computer Engineering Department faculties in the University of Denver since they have provided me with all information which assisted me in my Master's degree either for course work or my research. Finally, I dedicate this work for my parents, my wife and my kids as they assisted me to finish my degree and overcame all challenges.

Table of Contents

1 Chapter One: Introduction 1
1.1 Overview of Microgrids 1
1.2 Microgrid Projects in the US 3
1.3 Microgrid Challenges 9
1.3.1 Technical challenges. 10
1.3.2 Economic challenges. 11
1.4 Challenges Addressed by this Thesis 12

2 Chapter Two: Forecasting 13
2.1 Forecasting Overview 13
2.2 Forecasting Methods Classifications 17
2.2.1 Time scale classification. 17
2.2.2 Model input classification. 18
2.3 Examples of Some Methods 21
2.3.1 Models based on physical approach. 21
2.3.2 Models based on statistical approaches. 25
2.4 Recommendations for Wind Forecasting 29

3 Chapter Three: Unit Commitment 31
3.1 Electricity Market in the United States 31
3.1.1 PoolCo markets. 33
3.1.2 Bilateral contract markets. 34
3.1.3 Hybrid market. 34
3.2 Unit Commitment Definition 34
3.3 Unit Commitment Methods 35
3.3.1 Priority list method. 35
3.3.2 Dynamic programming method. 36
3.3.3 Lagrangian relaxation method. 36
3.3.4 Mixed-integer programming method. 37
3.3.5 Genetic algorithm method. 37
3.3.6 Simulated annealing method. 38
3.3.7 Particle swarm optimization method. 38
3.3.8 Tabu-search method. 38
3.3.9 Fuzzy logic method. 39
3.3.10 Hybrid methods. 39
3.4 Price-Based Unit Commitment (PBUC) 40
3.5 Security-Constrained Unit Commitment (SCUC) 42

4 Chapter Four: SCUC Modeling for Microgrids 43
4.1 SCUC Constraints for Microgrids 43
4.1.1 The load balance constraint. 43

4.1.2 Limits of generation units. 45
4.1.3 No load/start up/shut down indicators constraint. 45
4.1.4 No load cost. 46
4.1.5 Start up cost. 46
4.1.6 Shut down cost. 47
4.1.7 Reserve constraint. 47
4.1.8 Ramping up/down constraints. 48
4.1.9 Minimum up/down time constraints. 48
4.1.10 Main power flow constraint. 49
4.1.11 Main power flow fluctuation constraint. 50

5 Chapter Five: Numerical Analysis 52
5.1 Wind Forecasting Models 52
5.1.1 Preparing data for forecasting models. 52
5.1.2 ARIMA model. 53
5.1.3 ANN model. 55
5.2 SCUC Model 60
5.2.1 Preparing data for SCUC model. 60
5.2.2 SCUC cases. 62
5.2.2.1 Case 1. 63
5.2.2.2 Case 2. 70

6 Chapter Six: Conclusion and Future Work 76
6.1 Conclusion 76
6.2 Future Work 78

7 References 80

List of Figures

Figure 1-1: Typical structure of a microgrid 2

Figure 1-2: The infrastructure of the IIT microgrid 6

Figure 1-3: Kythnos island project 8

Figure 1-4: Solar cells on residential rooftops, Bronsbergen residential microgrid 9

Figure 2-1: Rooftop PV panels for a residential home 13

Figure 2-2: Wind farm 14

Figure 2-3: Artificial neural network 19

Figure 2-4: The flow chart of Landberg ‘s model 22

Figure 3-1: a) Vertically integrated utility. b) Horizontally integrated restructure (deregulated) 32

Figure 3-2: RTOs/ISOs in the North America 32

Figure 4-1: Simple structure of microgrid 44

Figure 5-1: The actual and forecasted wind power based on ARIMA (2, 0, 0) 54

Figure 5-2: NN toolbox start 55

Figure 5-3: Kinds of nonlinear time series problem 56

Figure 5-4: The training algorithm 57

Figure 5-5: ANN model 58

Figure 5-6: The actual and forecasted wind power data with ANN model 58

Figure 5-7: Comparison between ANN and ARIMA models with actual data 59

Figure 5-8: The commitment state of all units over 24 hours 65

Figure 5-9: The market price of the main grid power over 24 hours 66

Figure 5-10: The main power flow (3MW-wind turbine) 67

Figure 5-11: The main power flow (4MW-wind turbine) 68

Figure 5-12: The main power flow (5MW-wind turbine) 69

Figure 5-13: The main power flow for each fluctuation limit – 3MW-wind turbine 71

Figure 5-14: The main power flow for each fluctuation limit – 4MW-wind turbine 72

Figure 5-15: The main power flow for each fluctuation limit – 5MW-wind turbine 73

Figure 5-16: The total operating cost versus the fluctuation limits for all cases 74

Figure 5-17: The lost revenue versus the fluctuation limits for all cases 75

List of Tables

Table 2-1: NWP models 23

Table 2-2: Some of statistical models 25

Table 3-1: UC methods 35

Table 3-2: Comparison between PBUC and SCUC 41

Table 5-1: MAPE for different p and q orders 53

Table 5-2: The AR (2) coefficients 53

Table 5-3: The MAPE for ANN with different hidden layers 57

Table 5-4: Generators data 60

Table 5-5: The hourly load data 61

Table 5-6: The hourly main power market price data 61

Table 5-7: Actual and forecasted hourly wind data for 3MW, 4MW and 5MW wind turbine 61

Table 5-8: The total one-day operating cost for microgrid with a 3MW-wind turbine 63

Table 5-9: The committed state for the units with actual, ANN forecast and ARIMA forecast 64

Table 5-10: The units generation (MW) with actual, ANN forecast and ARIMA forecast cases 64

Table 5-11: The total one-day operating cost for microgrid with a 4MW-wind turbine 68

Table 5-12: The total one-day operating cost for microgrid with a 5MW-wind turbine 69

Table 5-13: The total cost for each forced limit when 3MW-wind turbine integrated with the microgrid 70

Table 5-14: The total cost for each forced limit when 4MW-wind turbine integrated with the microgrid 72

Table 5-15: The total cost for each forced limit when 5MW-wind turbine integrated with the microgrid 73

1 Chapter One: Introduction

1.1 Overview of Microgrids

Microgrid is defined by the United States Department of Energy (DOE) as:

> A group of interconnected loads and distributed energy resources within clearly defined electrical boundaries that acts as a single controllable entity with respect to the grid. A microgrid can connect and disconnect from the grid to enable it to operate in both grid-connected or island-mode [1].

Technically, microgrids consist of at least one distributed energy resource (DER) and one load demand which could be considered as small-scale power system connected to the main distribution grid. The microgrid is an autonomous system; so it can island itself from the utility grid during outage events and reconnect itself when the problem is solved. Due to this feature, microgrid is a very important technological development in modern power systems since it can potentially increase the power system reliability. In addition, it saves wasted heat since DERs will be placed near the heat loads using combined heat and power technology (CHP). The Point of Common Coupling (PCC) and the Circuit Breaker (CB), as shown in Figure 1-1, process the islanded mode and reconnected mode through power electronics. Implementing microgrids allows for a more economical power system. The cost of the transmission lines will be greatly reduced compared to current main grid systems since the generation will be close to electrical and heat loads [2]–[4].

There are many types of microgrids, e.g., they can be home microgrids that serve individuals directly and are owned by the homeowner. Or, they can be named after the type of the critical load supplied by them. For example, a hospital microgrid supplies a hospital or a campus microgrid supplies a university campus. The microgrid can be shared between groups of neighboring homes to supply their loads – a community microgrid.

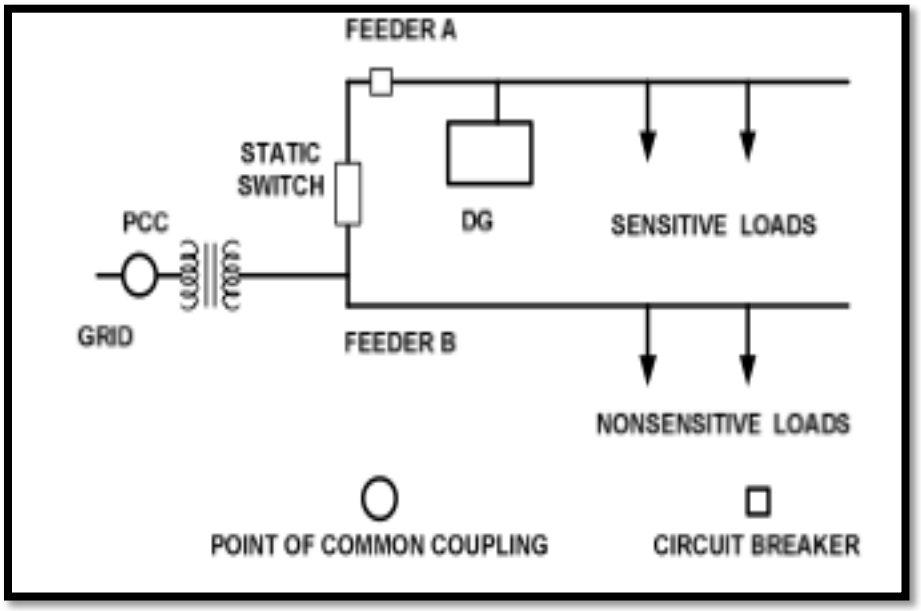

Figure 1-1: Typical structure of a microgrid [4]

DERs can be wind, solar, gas, or any other generation technology. Renewable integration is one of the benefits of using microgrids. By using renewable resources in microgrids, the environment will be less affected than using fossil fuel generation systems. Furthermore, utility emergencies, such as hurricanes, storms, or tornados, will not impact supply to microgrid customers as microgrids can be isolated from the main grid and operate in islanded mode. Moreover, customers will benefit from unused wasted

heat from microgrid generation to feed their heat loads. In main grid systems, the unused heat is wasted since heat is not transferable like electricity. In addition, the cost of transmission and distribution losses is dropped when microgrids are implemented. Microgrids do not need the transmission network because the generation units will be close to loads. As a result, microgrid technology no longer requires the transmission and distribution expansions of power systems. The overall energy consumption will consequently be reduced [4], [5].

1.2 Microgrid Projects in the US

Microgrids have received significant attention in recent years, especially from the research community. Many microgrid publications concentrate on microgrid operation, control and economic impacts of microgrid implementation. There are many completed and ongoing microgrid projects in the United States. Listed below are eighteen projects in the U.S. documented in [6]:

- Ansonia (Ansonia, CT)
- Borrego Springs (Borrego Springs, CA)
- Colonias (La Presa, TX)
- Drexel University (Philadelphia, PA)
- Fort Bliss (Fort Bliss, TX)
- Fort Bragg (Fort Bragg, NC)
- Howard University (Washington, D.C.)
- Los Alamos (Los Alamos County, NM)

- Marin County (San Rafael, CA)
- Naperville (Naperville, IL)
- New Mexico Green Grid Initiative (NM)
- Pecan Street Project, Inc. (Austin, TX)
- Perfect Power at the Illinois Institute of Technology (Chicago, IL)
- Perfect Power at Mesa del Sol (Albuquerque, NM)
- Sacramento Municipal Utility District (Sacramento, CA)
- Stamford Energy Improvement District (Stamford, CT)
- Twenty-nine Palms (Twenty-nine Palms, CA)
- University of California, San Diego (San Diego, CA)

Following are more details regarding some of aforementioned projects:

The mayor of Ansonia CT, announced plans to construct the Energy Improvement District (EID) in 2007. EID is a microgrid utilizing distributed energies. The goal of this EID was to allow local businesses to participate in a microgrid, providing a means of reducing consumed power cost and increasing power reliability. This decision may have been driven by the several day power blackouts of Connecticut's statewide local grid. After the announcement, the mayor received a commitment from Ansonia Copper & Brass, a famous company in microgrid technology. This commitment encouraged other companies to join in this important project with Ansonia Copper & Brass. The mayor of Ansonia consulted Pareto Energy, Ltd, a specialist in financing and designing Energy Improvement Districts, to develop the EID [7].

Fort Bragg in North Carolina has a microgrid project which is one of the largest projects in the U.S. This microgrid serves around 100 square miles of distribution network and utilizes a variety of distributed energy resources, such as diesel generators, fuel cells and gas turbines. There are fifteen diesel generators that together supply 8 MW of energy. Also there is a recently installed gas turbine, providing capacity of 5 MW, bringing the total microgrid capacity to 13 MW. In addition, it provides a single 5 KW fuel cell as storage [8].

The Los Alamos microgrid project is located in the mountain town of Los Alamos, NM. Startup of this project was with a $27 million investment. The contract to build this microgrid is cosigned by Los Alamos County, Los Alamos National Laboratory (LANL), the state of New Mexico and nineteen cooperating companies from Japan. This $27 million in contracts will be distributed to accomplish construction as follows:

- A 2-MW photovoltaic facility (solar power) on the top of the county's capped landfill.
- A 7-MWh-battery storage system.
- A smart house to demonstrate new construction techniques, smart meters and smart appliances [9].

Marin County's microgrid project includes 5 municipal departments in the city civic center, funded by Department of Energy's, Office of Electricity Delivery and Energy Reliability, Smart Grid Research and Development Program, Pacific Northwest National Laboratory (PPNL), and the Marin County Office of Sustainability. The project is implemented in four stages; each stage should use existing advanced software and

smart technologies. The target of this project is to allow utilities and customers to manage their distributed renewable energies and easily integrate them on power systems. The Marin County Energy Authority (MEA) spent $30 million to support the project demonstration on 1000 commercial building and 5000 homes in three Marin comminutes [10].

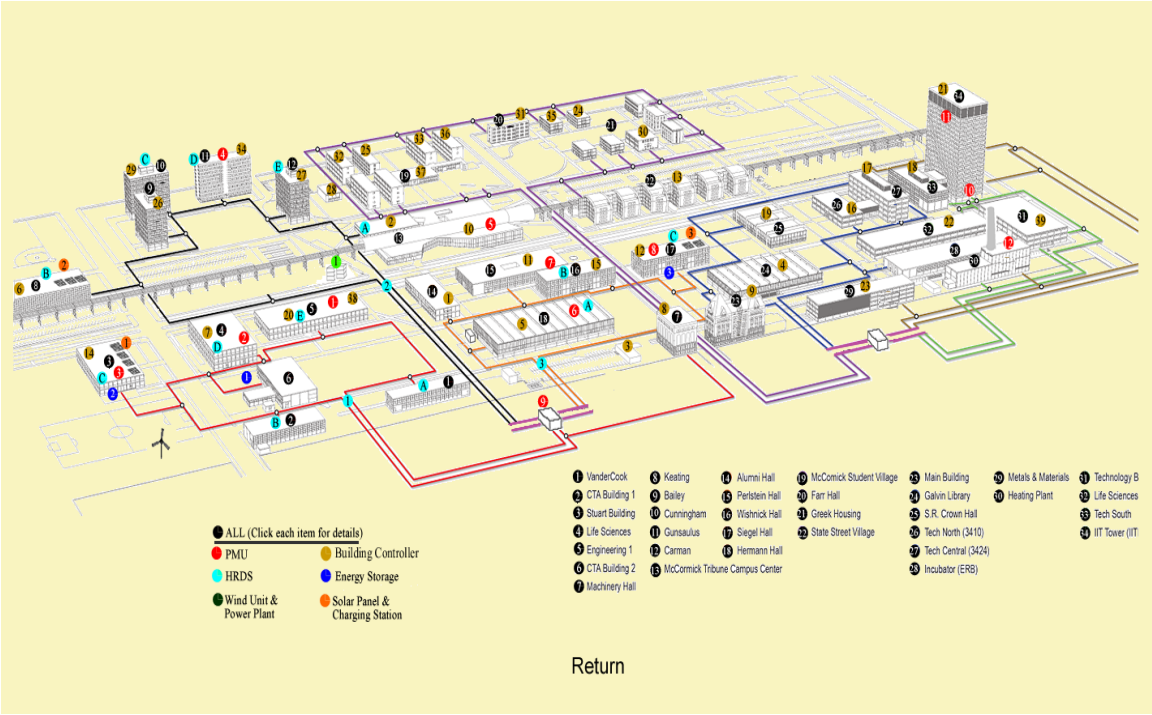

Figure 1-2: The infrastructure of the IIT microgrid [11]

Galvan Electricity Initiative conducts three projects in Illinois and New Mexico. These projects were built on Naperville and Illinois Institute of Technology (IIT) in IL and Mesa del Sol in NM. All these projects are founded under Perfect Power Systems. The Naperville project is set as a model of the electricity distribution systems and demonstrates how to maximize the power systems efficiency and quality. Galvan promoted this project by completing a case study exhibiting how projects of this type will

aid communities. IIT smart microgrid, Figure 1-2, was begun in 2006 and is considered as the first example of smart grids across the United States. IIT is facing three or more blackouts every year which annually result in an approximate financial loss of one half million U.S. dollars. As a result, they have planned to build this microgrid to reduce financial loss and to raise power reliability. IIT and DOE jointly funded this project through a $12 million investment. The payback period for this microgrid is five years including a one-time saving of $5 million and an additional $1.3 million each year. It provides advantages besides reducing IIT's energy bill and improving power quality, e.g., eliminating the need for grid upgrade or expansion, promoting a green environment and improving campus security. The Mesa del Sol project is developed by The Galvin Electricity Initiative, the state of New Mexico and their Green Grid Initiative, and Japan's New Energy and Industrial Technology Development Organization (NEDA). The payback of this microgrid is 30 years, much longer than IIT's microgrid [11]–[13].

The microgrid in the University of California, San Diego is located at its campus, an area of approximately 1200 acres. There are 450 buildings and a population of 45,000. The microgrid contains two gas turbines, each providing 13.5 MW of power. It also utilizes a steam turbine that provides 3 MW and a 1.2 MW installed solar unit. All of these resources can supply around 80% of the campus annual power demand. Because these turbines emit 75% less gas than conventional power plants, there is additional benefit of providing a healthier environment in the campus [14].

In Europe, there are many microgrid projects. For example, the Kythnos island project, built in Greece in 2001, supplies the power for 12 houses in a valley in

Kythnos. This microgrid contains a 10 kW solar power unit, a 5 kVA diesel generator, a battery bank of 53 kWh and three 4.5 kVA battery inverters, Figure 1-3. The Bronsbergen residential microgrid is another example of a European microgrid project, the first microgrid in Netherland. It has a total capacity of 315 kW powered by solar cells installed on the rooftops of residential homes, Figure 1-4 [15].

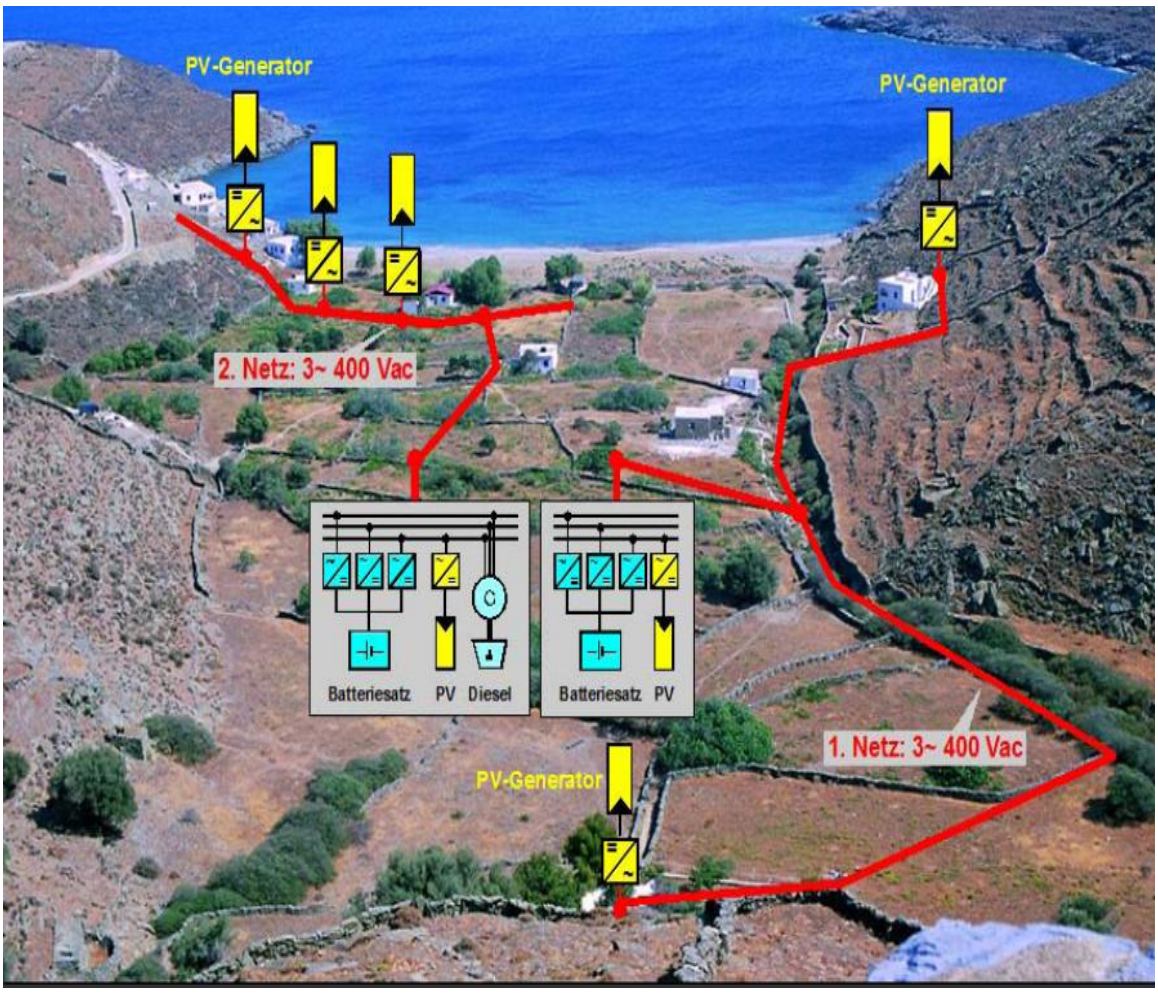

Figure 1-3: Kythnos island project [15]

Figure 1-4: Solar cells on residential rooftops, Bronsbergen residential microgrid [15]

Researchers optimistically forecast rapid microgrid implementation in all distribution networks worldwide, such as homes, neighborhoods, educational institutes, hospitals and all other applicable places whether or not they are critical.

1.3 Microgrid Challenges

From development through implementation, microgrids have faced many challenges. Some of these challenges are technical and others are economical. Both issues will be discussed respectively in the following.

1.3.1 Technical challenges.

There are many technical challenges involved in microgrid implementation. The control, operation and protection of microgrids are three greatest technical challenges, especially in islanded operation mode. One of the control challenges of microgrid is voltage and frequency control. A second challenge is the autonomous operation of the microgrid. Another is the microgrid protection.

It is very challenging to operate more than one distributed energy resource with different generation types (PV, wind, fuel cell, micro turbine, etc.). The active and reactive power might be unbalanced with consumed power. This unbalance causes a difference in the system frequency from its setting point (50/60 Hz) because of voltage and frequency drops during the islanding from the main grid. However, it is difficult to control reactive and reactive power through an active and reactive power controller because of the vast number of different generation resources. Therefore, it is a challenge to control these drops through the use of power electronics. Active power versus frequency drop is a method to control the frequency drop by controlling the power sharing among the DERs. In like manner, reactive power versus voltage drop is used to control the voltage drop. In addition, it is a more significant issue to ensure the autonomous operation in microgrid. It is an even more of a challenge to operate different types of distributed generation in autonomous mode operation because microgrid needs two interface controls, one for the normal operation (grid connected) and the other for islanded operation (grid disconnected). Using power electronics, such as inverter controls, is one method of overcoming this obstacle. Finally, microgrid protection

poses another challenge. It is important to ensure loads, DERs and all lines are protected when implementing a microgrid as a reliable and high quality power system. Power electronics should also be involved to ensure success in microgrid protection [15], [16].

1.3.2 Economic challenges.

The economics related to any project are primary concerns. Reducing cost and raising reliability of power through the use of microgrid technology is one manner of addressing these economic concerns. The difficulty of obtaining optimal reliability and power quality from utilizing the microgrid receives much focus from technical papers and reports. One solution to this issue is scheduling microgrid islanding/reconnecting from/to the utility grid to obtain an optimal least cost operation. Microgrid scheduling can be accomplished through solving the unit commitment problem. Moreover, since renewable resources are among microgrid DERs, wind and solar power deployment in microgrids becomes a big economic issue because of unpredictable nature which is dependent on environmental factors, such as wind speed and sunshine. To obtain an economic advantage, it becomes essential to develop a reliable method for predicting the available power from wind turbines or solar cells. Getting an accurate renewable energy forecast is considered as a primary step before solving the microgrid unit commitment problem [15], [17].

1.4 Challenges Addressed by this Thesis

This thesis addresses the economic challenges of integrating wind power in microgrids. It is difficult to integrate an unpredictable power source such as wind power into a microgrid with other DERs. To ensure an economic deployment of wind power into a microgrid, it is essential to develop a method for reliably and accurately forecasting wind power across a specific period of time, following which the challenge of solving the unit commitment for microgrids, which have a wind turbine as DER, is discussed. As the changes of the market prices and the total operating cost of the microgrid may cause fluctuation in the main grid power flow, a new constraint is proposed in security-constrained unit commitment (SCUC) to overcome this fluctuation. The new constraint is imposed by the main power utility. The options of how to impose the constraint are explained in chapter four.

The rest of the thesis is organized as follows: Wind forecasting and its methods and classification are discussed in Chapter 2. Chapter 3 provides a review on electricity market and unit commitment (UC) problem. SCUC modeling is presented in Chapter 4. Some cases providing numerical analysis about forecasting models and SCUC is presented in Chapter 5, and the conclusion and recommendations for future development are provided in Chapter 6.

2 Chapter Two: Forecasting

2.1 Forecasting Overview

The entire world is looking forward to have a clean environment and life without pollution. As a result, researchers and scientists are searching for alternative resources to help mitigate the impacts introduced by traditional energy resources. For instance, hybrid (electric and natural gas or propane) cars are available in the market to replace some fossil fuel automobiles, which help to reduce the carbon footprint of the transportation sector.

Figure 2-1: Rooftop PV panels for a residential home [18]

Similarly, researchers in the energy sector are giving more attention to renewable resources for generation of electricity to further reduce the effect of fossil fuel use on our environment. They understand that the reserve of fossil fuel is limited but the demand for energy is expected to increase over time and believe it is essential to find a sustainable and environmentally friendly energy resource. Renewable energy resources are gaining popularity as a potential solution to this problem.

Potential resources of renewable energy are hydro, solar, wind, biomass, and geothermal. Of these, solar and wind power are the two most common technologies attracting researchers across the globe.

Figure 2-2: Wind farm [19]

Solar power depends on weather and other specific factors related to the sun. The most important of these is sun radiation and its angle. Through a specific procedure, sunlight can be converted to electricity via photovoltaic (PV) panels, now apparent in the street or on rooftops in some countries, see Figure 2-1. In the United States, the

government encourages people to cover the rooftop of their home with PV panels to help them supply their electrical demand by clean energy, often through the provision of economic assistance or reimbursement.

Wind power is influenced by the wind speed and its direction. It is generated by wind turbines (commonly in wind farm settings, Figure 2-2). Wind farms are found in many locations in Europe. For example, in Spain, approximately 4% of the load is supplied from wind power generation. There are also wind farms in Colorado close to the Rocky Mountains. Wind turbine converts the wind energy to power through its power characteristic curve [20].

Utilizing wind to generate power has the lowest generation cost among other generation units, as the source is free. As a result, wind is one of the most beneficial renewable energy resources since it is the largest available pollution-free resource and because of its economic impact. Today, most countries are considering wind power generation as the first priority to develop. Consequently, wind energy is growing fast over the entire world. The total wind capacity in China is increased around 108% from 2008 to about 13 GW in 2010 [21]. As per wind energy and green peace organization forecast, wind power will generate 12% or more of all power generation in China (around 30 GW) by 2020 [22]. In addition, it is expected that future wind power generation will reach nearly 20,000 TWh/year, globally. When this huge amount of wind power is utilized, wind power will become a major contributor to the world's power generation and provide a major impact in helping to balance the power generation necessary to meet the worldwide power consumption needs [23].

In this thesis, the concentration is on wind power implementation in microgrids. The rapid evolvement of wind power integration in power systems is a major concern with power researchers since wind power is affected by wind speed. Wind speed is influenced by climate conditions such as temperature and barometric pressure and by topography and obstacles. Fluctuation in wind speed cannot allow wind energy to be utilized as a reliable energy source; it is not a steady enough resource to supply a steady supply and to meet a constant demand. One of the biggest challenges with implementing wind power into power systems is not knowing the power generation in advance. These issues with wind power implementation become problems with operation and maintenance scheduling, power system stability and reliability, power system planning, market pricing, ancillary services and power reserve capacity [22].

The forecasting of wind speed and wind power are exactly the same as the wind speed can be easily converted to wind power through the following equation [24]:

$$P = \frac{1}{2}\rho A v^3 \qquad (1)$$

Where P is the wind power in watts, A is the area of the selected region in square meters, and v is the velocity of the wind speed in meters per second. The density of the air (ρ) kg/m depends on the temperature and pressure of air. However, due to the cubic relation between wind power and wind speed, a small error forecast in wind speed might cause a large error in wind power [24].

2.2 Forecasting Methods Classifications

Wind speed generated wind power needs an accurate forecasting method to overcome all or most of above-mentioned implementation challenges. There are many forecasting methods recently developed by researchers. Most researchers classified the forecasting methods in one of two ways. The first way considers time horizon forecasting and the second, a forecasting model input [20], [24].

2.2.1 Time scale classification.

Time horizon forecasting methods are divided into four categories:

- Very short time forecasting:

  This forecast category is for about 30 minutes ahead. It is an aid to setting regulations, actions and electricity market.

- Short term forecasting:

  This forecast category spans 30 minutes to one day ahead and is used in planning of economic dispatch and load change decisions.

- Medium term forecasting:

  This time horizon forecast could begin at one day and span up to several months ahead. In this category, wind power forecasts help in power system operation, such as unit commitment, security operation of the power system, and maintenance scheduling.

- Long term forecasting:

  This is last time horizon category and it could be extent from several months to several years. Utilizing this category, power system operators can make reserve capacity decisions associated with system generation, transmission, and distribution expansion [24].

2.2.2 Model input classification.

Based on the model input, forecasting methods are divided into four categories:

- Persistence forecasting approach:

  This is also called "Naïve Predictor". It employs only the past or historical data of wind speed to forecast the future wind speed. It forecasts the wind speed at a specific time 't' to the same wind speed at the time 't-Δt'. This method is accurate when used on very short time horizon scales. Therefore, researches always compare their developed forecasting methods performance against the persistence method performance to evaluate the forecasting performance [24].

- Physical forecasting method:

  Physical forecasting method, also known as deterministic method, utilizes physical atmospheric conditions to predict future wind speed and direction. The numerical weather prediction (NWP) is the most widely known model based on a physical approach. NWP uses complex mathematical models. These models take the weather data as model input such as temperature, pressure, surface roughness,

description of orography, obstacles and so on. Models based on physical methods need more time to gather needed inputs resulting in delays in output results. Accordingly, NWPs benefit from better accuracy with long term forecasting than other time scale forecasting. When the weather situations are unchanging, the NWP models can provide more precise forecasting [20], [22], [24].

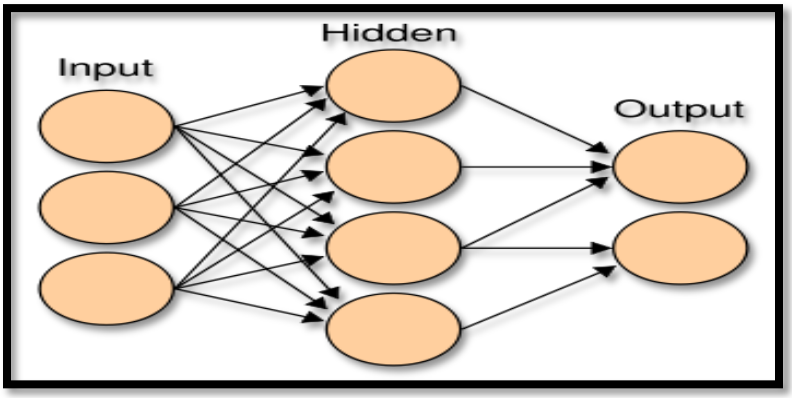

Figure 2-3: Artificial neural network [25]

- Statistical forecasting approach:

  This approach is split into two subclasses. The first subclass is artificial neural network (ANN) model, Figure 2-3, and the second subclass is time series model. An ANN forecasting approach utilizes massive amounts of past wind speed data to predict upcoming wind speed. This method is capable of providing a timely predication based on historical data time series. It does not consider weather conditions but rather the time series history of wind speed on a specific selected area. The statistical models operate based on a number of mathematical equations defined by identifying the pattern of time series of past data. The statistical models are easy to model and less expensive than other models. Their accuracy or performance is great when the parameters are accurately tuned to meet the

pattern of past data time series. In this forecasting method, neural network (NN) models usually provide superior accuracy compared to time series models, but there are some very good time series models which outperform ANN models [20], [24].

- Spatial correlation methods:

  Spatial correlation modeling is more difficult than other forecasting models as it employs the spatial relationship of wind speed or wind power of neighboring sites. The models based on spatial correlation often achieve high prediction precision. Also, this kind of forecasting has employed various other intelligent technologies such as ANN, fuzzy logic and Kalman filter [20], [21]. It is more useful to use spatial correlation for predicting wind farm output since the total wind power of the wind farm could be correlated with the wind speed at one or more reference points in the wind farm rather than wind speed data from the entire farm area [26].

More recent methods study the combination of two forecasting models. These studies have evolved into a new forecasting approach, the hybrid forecasting method. Hybrid methods can be a combination of physical approach model and statistical approach model or between two models that are both from same approach. Moreover, it might be a mixture between short term and medium term forecasting approaches [24].

2.3 Examples of Some Methods

Several publications study forecasting approaches and show their results. Many papers are published regarding physical and statistical approaches. Following is a review of both physical and statistical approaches.

2.3.1 Models based on physical approach.

NWP is mostly based on weather data. Furthermore, NWP models provide not only wind speed forecast but a detail forecast output as well. For that reason, they are not only used for power forecast, but also for various applications [27]. These models are usually used in new wind farms since they do not need a history data to use [28]. There are many models that are based on physical methods or NWP Models. Some of these models work well for short term and others are better with long term forecasting. Beyond this, some of them are regional models and others are global.

The NWPs sometime need to operate with other models to obtain more accurate performance. For example, in order to represent the topography of the area, NWP must use digital elevation models (DEMs). NWPs must then utilize model output statistics (MOS) to reduce forecasting errors [20].

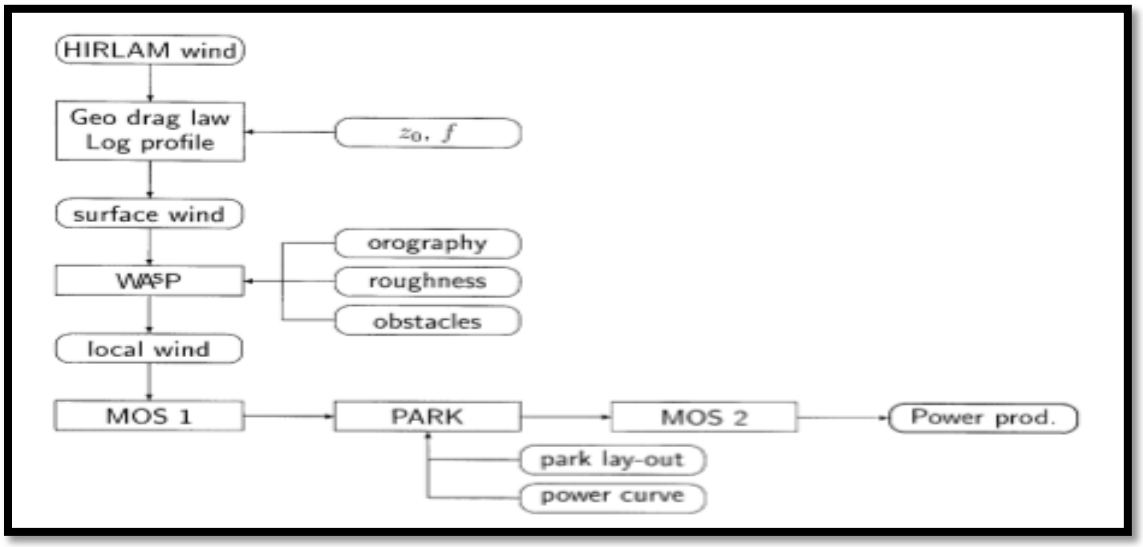

Figure 2-4: The flow chart of Landberg ‘s model [29]

In [29], a model (High-Resolution Limited Area Model - HIRLAM) was used. HIRLAM is created and developed by Denmark meteorologist institute and European meteorology institutions. To test the model, data spanning one year from February 1995 to January 1996 was used by selecting 17 wind farms at Danish isles Zealand and Bornholm, with a total wind power capacity of 35.7 MW. More data was needed to support the large-scale flow. This data was supplied through wind atlas analysis and application (WAsP) program. Also, the PARK program was used to take into account shadow effects of the turbines. At the end, model output statistics (MOS) was used to reduce output error results. The model, Figure 2-4, was designed to provide a 4-hour to 36-hour forecasting. It was operated twice daily in a grid of 162×136 points with spacing of 26 km and 16 vertical levels. Results from this model demonstrated that for the first 4 hours the persistence method performed better than this model. Therefore, it is not recommended to use this model with short term forecasting since other statistical

methods yielded better accuracy with a very low incidence of forecasting error. Some of NWP models are listed in [27] and provided in Table 2-1.

Table 2-1: NWP models [27]

Model name	**Developer**
GFS	National Oceanic and Atmospheric Administration (NOAA), US
ARPEGE	Metro-France
GME	Deutscher Wetterdienst (DWD), Germany
GEM	Recherche en Prévision Numérique (RPN), Meteorological Research Branch (MRB), and the Canadian Meteorological Center (CMC)
UM	Met Office, UK
GSM	Japan Meteorological Agency (JMA)
LM	DWD, Germany
WRF	A collaboration in the US, which includes NCAR, the National Oceanic and Atmospheric Administration (National Center for Environmental Prediction (NCEP) and the Forecast Systems Laboratory (FSL)), the Air Force Weather Agency (AFWA), the Naval Research Laboratory (NRL), the University of Oklahoma and the Federal Aviation Administration (FAA)
COSMO	A collaboration of 6 European met services led by the Federal Office of Meteorology and Climatology MeteoSwiss

In addition, eight models based on NWP (HIRLAM and UK MESO) models and neural network model were developed in [20]. All eight models were compared with the persistence method and learned that all eight models performed better than the persistence method. However, the persistence method outperformed all eight models when considering short prediction time horizon (3-6 hours). Authors discovered the neural networks did not yield an exceptional contribution.

In [30], another kind of NWP models was used, Bologna Limited-Area Model (BOLAM). This model has been developed at the Institute of Science of Atmosphere and Climate (ISAC) and the National Research Council (NRC) in Bologna, Italy. This model was designed to be a grid-point hydrostatic model in sigma coordinate with variable spacing in vertical. There are many versions of developed BOLAM with variety of spatial horizontal resolution. The method was elected to work with the highest resolution of BOLAM 7 and a horizontal grid distance of 7 km. The data set used in the study was a two-year span from 1 January 2007 till 31 December 2008. The data was gathered from several wind farms, Lago di Giacopiane, Casoni di Suvero and Varese Ligure. The Varese Ligure wind farm has four wind turbines with a total power of 3.2 MW of which only two of them that are NEG MICON 1 and NEG MICON 2 turbines were considered. It was learned that the NWP BOLAM standing alone provided poor forecasting performance. However, when the BOLAM model output was used with a Kalman filter, a significant improvement of the wind power forecast compared with the direct NWP BOLAM model would be observed. As a result, combining Kalman filtering with NWP direct outputs provided a high accuracy forecasting and contributed to improve the NWP model outputs. These findings exhibited that the integration of wind power into the microgrid could potentially improve the process as wind forecasting became more reliable.

2.3.2 Models based on statistical approaches.

Researchers have increased their interest in statistical approaches as a means to forecast wind power generation because this approach depends solely on the historical wind speed or wind power generation, unlike physical approaches. Hence, there are many papers about the statistical approach, especially for short and medium term forecasting.

NWP output often comes as an input to these models. Statistical approaches only need one step to convert inputs to forecasted wind power; because of that, they are also termed 'black box'. The general principle of these methods is in discovering the link between past wind power production data and past wind speed data. In other words, identifying the pattern of historical values of the wind power time series and then forecasting the future based on that pattern [27].

Table 2-2: Some of statistical models [27]

Model name	**Developer**
WPPT	Eltra/Elsam collaboration with Informatics and Mathematical Modeling at Danmarks Tekniske University (DTU), Denmark
Sipreólico	University Carlos III, Madrid, Spain & Red Eléctrica de Espana
WPMS	Institute für Solare Energieversorgungstechnik (ISET), Germany
GH	Garrad Hassan
AWPPS	École des Mines, Paris
Alea Wind	Aleasoft at the Universitat Polytécnica de Catalunya, Spain (UPC)

As mentioned above, the statistical methods have two subcategories: time series models and artificial neural network models. These two subcategories have many models, such as, autoregressive (AR), Moving average (MA), autoregressive-moving

average (ARMA), autoregressive integrated moving average (ARIMA), the Box-Jenkins method, Kalman filter, learning approaches (artificial intelligent - AI), fuzzy systems, gray predictor, support vector machines and so on [27]. Some of statistical models are listed in [27] and provided in Table 2-2.

Artificial intelligence is also known as the learning approach method, which learns the relationship between wind speed and output of wind power through observing the past data from a time series of both. Artificial neural network methods are also called data-driven methods because they learn from data experience. NN models, which are multi-layer perception (MLP), are often used in research case studies [27].

ARMA is the best-known approach based on time series to predict potential wind speed or wind power. Also, ARIMA can be another form of ARMA but including integrating parameter (*d*). (2) shows the general model for ARMA (*p, q*) where *p* represents the order of autoregressive part and *q* is the order of moving average part.

$$x_t = \sum_{i=1}^{p} \varphi_i x_{t-i} + \sum_{j=1}^{q} \theta_j \alpha_{t-j} + \alpha_t \qquad (2)$$

Where φ_i , θ_j are the autoregressive parameter and moving average parameter, respectively, x_{t-i} represents the past value of forecasted wind speed or power at time *t* (x_t) and α_t is the normal white noise time series with mean average of 0. When integrated part (*d*) is included, the ARIMA (*p, d, q*) would be considered with its parameter *d*. In this thesis, only ARMA (*p, q*) will be used for wind power forecasting [20].

In [31], four distinct approaches were used to predict wind speed and its direction. These approaches are: the component model, combined traditional ARMA model and linked ARMA model, the vector autoregressive model (VAR) and another one descended from the third with some parameters assigned 0 value. It is also demonstrated the method to model each approach starting with determining the autoregressive and moving average orders *(p, q*). The ARMA orders can be achieved by using the auto correlation function (ACF) and partial auto correlation function (PACF) plots. In the component approach, the mean of wind direction ($\bar{\theta}$) and the lateral and longitudinal component of wind speed (v_x, v_y) were found. Then the forecasted wind speed (v) and direction (θ_t) were found simultaneously by using (3) and (4).

$$\theta_t = \tan^{-1}\left(\frac{v_x}{v_y}\right) + \bar{\theta} \quad (3)$$

$$v = \sqrt{v_x^2 + v_y^2} \quad (4)$$

In the combined traditional ARMA model and linked ARMA model, traditional ARMA model was used for forecasting the wind speed and the linked ARMA model for forecasting the wind direction. The first step was to forecast the linear variable (wind speed), and then converted the linear variable to circular variable (wind direction) by applying the linked ARMA model. From this process, the forecast of wind speed and direction was obtained. The third and fourth approaches were based on the vector autoregressive model (VAR), VAR was selected since it is another form of persistence method which already includes wind direction forecasting. The fourth approach is called restricted VAR. The data was gathered at a wind observation site in North Dakota

between May 1 and October 21, 2002. The models performance was determined by measuring the mean absolute error (MAE).

Following is the conclusion reached from the study. For wind direction, the component model outperformed the other three models while the traditional-linked ARMA model exhibited the worst results. By comparing the VAR and restricted VAR, VAR marginally performed better than the restricted VAR. However, restricted VAR model was preferred as it requires fewer parameters than VAR model. For wind speed, the traditional-linked ARMA model, VAR model and restricted VAR model performed better than component model, observing that the performance was similar, but slightly better performance of traditional-linked ARMA model compared with VAR and restricted VAR models.

Hybrid forecasting methods are receiving more attention. In [32] this method was used for wind forecasting in three different areas in Mexico, the Isla de Cedros in Baja California, the Cerro de la Virgen in Zacatecas and Holbox in Quintana Roo. The proposed method combined the ARIMA and ANN models. The hourly average time series historical data gathered from these different sites over the period of one month. Part of the data was used for validating the model. Using the ARIMA model for all regions, the best results were obtained with ARIMA (1,0,0), ARIMA (2,0,0) and ARIMA (2,0,0) for the Isla de Cedros, the Cerro de la Virgen and Holbox, respectively. The authors first utilized the ANN model. The number of input vectors, the number of output vectors, the number of layers and the number of neurons must be specified at first, commencing with the simplest model configuration then toward the more

complicated configurations. Consequently, the following model configurations were selected: 2-layers and 3-nerurons, 2-layers and 4-nerurons, 3-layers and 6-nerurons, 3-layers and 7-nerurons. After testing all these model configurations with wind forecasting in the Isla de Cedros, it was found that the simplest configuration, which is 2L-3N, provided the best result. After testing ARIMA and ANN separately, the authors decided to combine both models into a hybrid model. The accuracy was measured by calculating three forecast error methods to compare all models - the mean error (ME), the mean square error (MSE) and the mean absolute error (MAE). The conclusion revealed that the output result of all models exhibited a reasonable performance with following the time series. However, the hybrid model provided higher accuracy prediction than ARIMA and ANN models in all three selected regions.

2.4 Recommendations for Wind Forecasting

Below are recommendations on wind forecasting, summarized on the following points:

- Specify the forecasting purpose.
- Select the time horizon for forecasting depending on the purpose. For instance, if the forecasting purpose is power system planning, it is better to forecast for long term. However, it is better to forecasting short term for operation purposes.
- Select the appropriate forecasting method depending on the forecasting purpose and the time horizon.

- Use different data sets to test the forecasting model - some models are sensitive to the input data.
- Examine your model in different areas as an accuracy check.
- Calculate different forecast error measures for each model to get a clear result for its accuracy (i.e. ME, MSE, MAPE, MAE…etc.).
- Reduce the forecasting error by employing the hybrid method; since all combined models have given more accurate forecast than single models that forms the hybrid models.

3 Chapter Three: Unit Commitment

3.1 Electricity Market in the United States

Traditionally, in power systems the electricity is generated, transmitted and distributed by the public power utilities under regulated environment. The energy infrastructure later changed to deregulated and privatized market to increase competition and enhance quality of service. The electricity market is commonly divided into three sectors as shown in Figure 3-1 and listed as follows:

- Generation companies (GENCOs) generate electricity,
- Transmission companies (TRANSCOs) transfer the electricity to the distribution grid
- Distribution companies (DISTCOs) deliver the electricity to the customers.

All these companies manage their duties independently unlike the vertically integrated structure. In other words, the market became decentralized as any supplier can easily participate in it. As a result, the Federal Energy Regulatory Commission (FERC) established Independent System Operators (ISOs) to run the energy markets in various regions. ISOs are similar to Regional Transmission Organizations (RTOs), but RTOs are wider as they encompass all North America energy markets (the United States and Canada) whereas the ISOs are limited to the United States markets. There are seven

ISOs in the United States as described in Figure 3-2. Regions, not assigned to any ISO, are still working with vertically integrated structure. ISOs are responsible to ensure open access to the transmission grid. The driving force behind this change is to eliminate market monopoly and open the energy market for competition. As a result, the energy price lowers and benefits the energy consumers [33], [34].

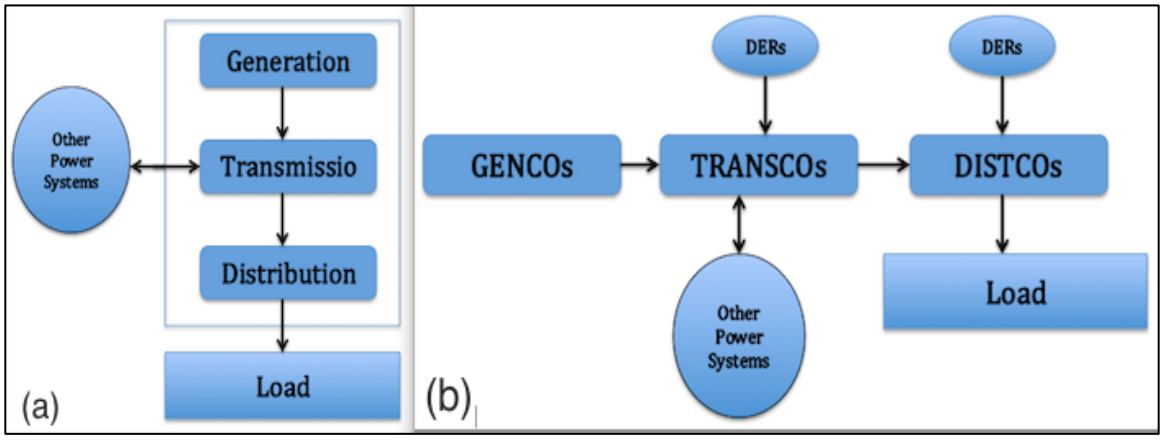

Figure 3-1: a) Vertically integrated utility. b) Horizontally integrated restructure (deregulated)

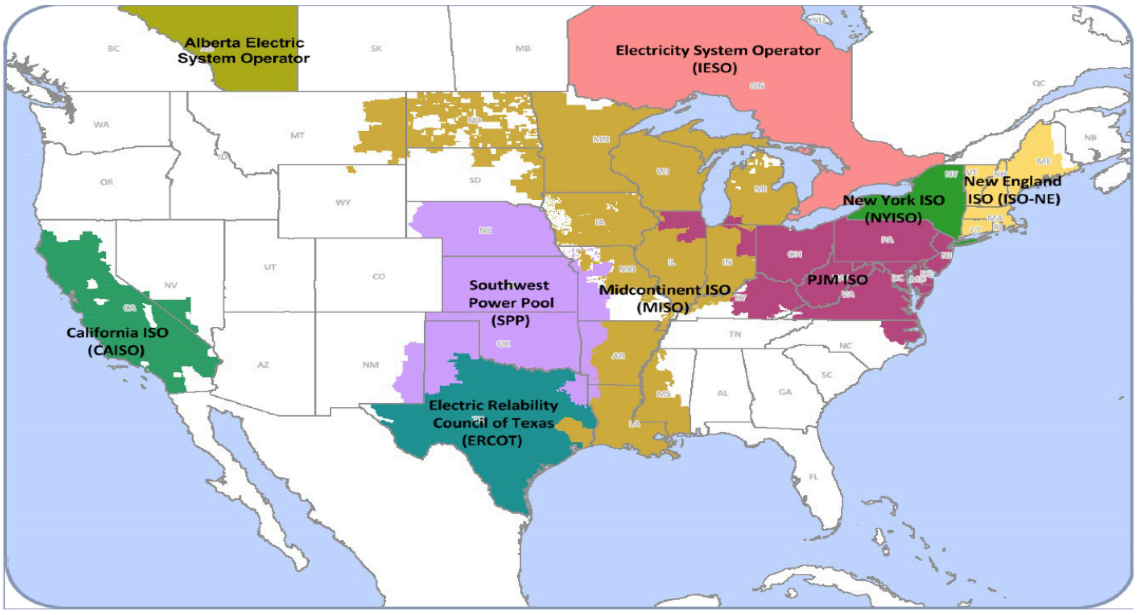

Figure 3-2: RTOs/ISOs in the North America [33]

In the deregulated structure, ISOs receive generation bids from GENCOs while the system operators in vertically integrated systems receive the fuel cost curves from generation units. The generation cost in vertically integrated systems is calculated based on the fuel cost, but in the deregulated environment it is based on the biding curve. The energy markets in the United States are divided into two market designs. These two designs differ depending on the participants, the information that are shared between the ISO and the participants and the responsibilities of the ISO in the markets. These markets are called PoolCo market and bilateral contract market [35].

3.1.1 PoolCo markets.

This market design is a centralized wholesale market run by the ISO. In this market, the suppliers or GENCOs send their bids to the ISO including the amount of power they are willing to deliver to the market and bid-cost curves. ISO could also receive the demand bids at the same time. Then ISO will decide the amount of power to be generated by each generation unit depending upon total market information received from all market participants. ISO must remain independent of all market participants to manage the market and assure it is competitive. If the suppliers bid a high cost, their power may not be purchased since the probability to get better price is high. Similarly, the consumers may not be able to purchase the power when their bids are very low [35].

3.1.2 Bilateral contract markets.

A Bilateral contract market is a contract between two parties who negotiate and agree its rule together, independent of the ISO. Thus, the supplier and the consumer agree on the amount of delivered and consumed power and also the energy price. Despite of this market being independent of ISO; this information should be sent to the responsible ISO to check the required transmission capacity to execute the contract and maintain the transmission grid security [35].

3.1.3 Hybrid market.

Hybrid market either chains the above two market options together or utilizes a combination of most of their structures. Customers may select any supplier to deliver the power and negotiate the price directly with the supplier or they have the option to simply accept the power at spot market prices offered by PoolCo. However, PoolCO is responsible to serve all market participants who have not signed a bilateral contract with another party. This option is more flexible than the other two options as it uses the both options in one market. For this reason, customers prefer to be involved in hybrid market option [35].

3.2 Unit Commitment Definition

Unit Commitment (UC) problem finds the optimal hourly schedule, i.e., commitment and dispatch, of generation units, considering system and units constraints. The goal of the UC problem is to minimize the total operating cost and satisfy the system

security by meeting all constraints. The accurate UC depends on the accuracy of load forecast and renewable energy forecast in case of renewable energy integration. The UC problem can be solved for a duration of one day to one week depending on the application [36]–[38].

3.3 Unit Commitment Methods

UC methods are classified under three main groups: Deterministic, meta-heuristic and hybrid methods. Each group consists of different methods as shown in Table 3-1 [36], [38].

Table 3-1: UC methods

Main Methods	**Sub-Methods**
Deterministic Methods	Priority List (PL)
	Dynamic Programming (DP)
	Lagrangian Relaxation (LR)
	Mixed Integer Programming (MIP)
Meta-heuristic Methods	Genetic Algorithms (GA)
	Simulated Annealing (SA)
	Particle Swarm Optimization (PSO)
	Tabu-Search Method (TS)
	Fuzzy Logic Algorithm (FL)
Hybrid Methods	Memetic Algorithm (MA)
	Fuzzy DP
	ANN-DP
	Multi-Agent System (MAS)

3.3.1 Priority list method.

The priority list method (PL) is the easiest UC method to use and takes less time to solve the UC problem than other methods. However, the solution is not accurate and

optimal as some constraints are not considered in the priority order, such as start-up cost and the unit ramp rate. This method lists all the units regardless of its commitment state. It is then necessary to list the cost of each unit in order to establish a rank table for all units. After that, the system operator makes a decision of which unit should be committed according to the ranking table. The initial solution is crucial in this method and it may be generated randomly. All other solutions can then be compared with the initial solution to assist in forming a decision. The system security may not be met by this method, but only the sensitive loads can be secured by committing the units. This may result in obtaining an uneconomic solution for the UC [36], [38].

3.3.2 Dynamic programming method.

Dynamic programming (DP) is more flexible than the PL method. Nevertheless, it takes more time to solve the UC problem as the processing time is exponentially related to the problem size. When the dimension of UC problem is increased, the mathematical complexity is increased. As a result, the computation time of UC solution is increased and may reach a level that cannot be solved or computed [36], [38].

3.3.3 Lagrangian relaxation method.

Lagrangian relaxation (LR) is one of the most widely used methods for solving a UC problem. It is a successful method when applied to a complex UC which has many hard constraints, such as ramping up and down and minimum up and down constraints. Moreover, while it provides an acceptable solution, it may experience convergence

issues. The dual solution is not an optimal solution. The duality gap or the difference between the two solutions is small (1-2)%, while it was considered acceptable before energy markets changed to a more competitive market [36].

3.3.4 Mixed-integer programming method.

The mixed integer programming (MIP) method is a special class of linear programming. It is also known as mixed integer linear programming (MILP). MILP is one of the most useful and viable solution methods for solving UC. Since 2006, MILP has been by PJM ISO to improve the day-ahead market clearing process. Following the PJM experience, many ISOs now utilize MILP in their markets. MILP applies two types of variables: Binary variables (0 or 1) to denote the commitment state (OFF/ON) of the units and continuous variables to represent the dispatch of the units. The MILP assures a convergence solution in limited steps, unlike the LR. MILP can handle large–scale UC problems [37].

3.3.5 Genetic algorithm method.

The genetic algorithm (GA) method is a powerful method for solving a difficult UC problem as it utilizes a mechanism of natural genetics. GA is a stochastic method that utilizes the variable constraints imposed on the power system due to the nature of energy resources. Utilizing this method, it is possible to reach a global minimum solution rapidly while allowing the inclusion of inequality constraints is also simpler [36].

3.3.6 Simulated annealing method.

The simulated annealing (SA) method is an optimization method, suggested by Kirkpatrick, Gelatt and Vecchi in 1983. This method is based on simulating the annealing of metals. By using this method, the solution of UC problems can be theoretically converged to an optimum one [36], [38].

3.3.7 Particle swarm optimization method.

The PSO method has many advantages, e.g., improving simulation time, acquiring an optimal solution and obtaining a feasible solution for the UC problem. It is also considered to be more capable than the GA method [36].

3.3.8 Tabu-search method.

Tabu-search (TS) is one of the stochastic optimization methods that are successfully applied together with combinatorial optimization problems. This method is proved useful in solving power system optimization problems such as UC and reactive optimization. TS is an iterative method utilizing a flexible memory system unlike GA and SA methods. It does have the disadvantage of requiring a lengthy time to get a global minimum solution. In addition, obtaining an accurate minimum solution for large power systems is less than optimal [36], [38].

3.3.9 Fuzzy logic method.

Fuzzy logic (FL) algorithm is a numerical algorithm, capable of describing a specific system and its response without a precise numerical formulation. FL method is also used for solving forecasted load schedules error but the error's complexity may impact this process. A paper by Kadam used FL method in 2009 to solve a short term UC problem in power generation. The method proposed in this paper was compared to the priority list method (PL) and reported that the FL outperformed PL especially in nonlinear and multi-constraints UC problems [36], [38].

3.3.10 Hybrid methods.

The initiative of utilizing a hybrid method is for combining two solving methods to solve the UC problem. The hybrid methods are used in order to provide a more accurate and higher quality solution of UC problems. These methods can manage a large number of constraints even if they are complicated. Some hybrid methods are memetic algorithm (MA), fuzzy DP, hybrid ANN-DP and multi-stage neural network-expert system. MA is a method which combines GA and a local search method. Fuzzy DP is a method which employs fuzzy logic for forecasting hourly loads. Then DP is used to solve the UC problem thus making the fuzzy DP more powerful than traditional DP. Hybrid ANN-DP is a method which combines ANN UC method and DP UC method. ANN is used first to solve for UC according to the demand response. Then dynamic programming is executed for the next stage when UC states are not positive. A multi stage neural network-expert system (MSNNES) method is a combination of ANN and ES

methods. ANN is used for pre and post processing stages whereas the operating constraints are presented by the ES method. Moreover, GA, TS and SA are being used in hybrid methods for solving the UC problems [38].

There are two types of unit commitment in the electricity markets in the United States. These types are Price-Based Unit Commitment (PBUC) and Security-Constrained Unit Commitment (SCUC). Each type has its own hard constraints. Details regarding each type are as follows:

3.4 Price-Based Unit Commitment (PBUC)

This type of UC is mainly utilized by individual GENCOs. The main objective of PBUC is to minimize generation resources in order to maximize the GENCO's profit. It is termed price-based to underscore that the price signal controls the decision of the unit commitment state (which unit should be OFF and which ones should be ON). In PBUC, each individual supplier is responsible for its own strategies when bidding on the energy markets. Thus, the bidders bear the risk of their decisions when committing their units. GENCOs' aim is to get their profit maximized as much as they can disregarding the total system profit. Therefore, the load satisfaction is not as important in PBUC as it is in the SCUC. To avoid the hazard of not knowing the GENCOs' dispatched hours or the market clearing prices (MCPs), GENCOs send their single part bids to the responsible ISO. Thus, the ISO can maintain the system security by using this information to determine the MCP since the ISO's aim is the system security. However, GENCOs' aim differs because they are only concerned about their profit. By comparing PBUC with SCUC, it may be

argued that minimizing the total cost is similar to maximizing the profit. This is not precisely correct since the profit does not depend only on cost; it is more accurately calculated considering revenue minus cost. For that reason, when incremental revenue is larger than incremental cost, it becomes more attractive to generate more power and thus increase profit. On the other hand, GENCOs are not willing to sell energy if the incremental revenue is below the incremental cost. PBUC is also differs from the SCUC because the latter includes the transmission constraints. PBUC cannot include transmission constraints in cost forecasting as the transmission information is not available for GENCOs. SCUC is able to include these constraints because of the availability of transmission information to ISOs. A feature in PBUC is that the market price reflects all market information. Security is not considered in the PBUC formulation, but the ISOs' way of maintaining system security impacts the market price. PBUC can maximize the value of generation resources which is significantly essential in power generation [35], [38].

Table 3-2: Comparison between PBUC and SCUC

	PBUC	**SCUC**
Main objective	Maximizing the profit	Minimizing the cost
Load	No-obligation	Must be balanced
Security	Not included	Included as a hard constraints
Market Price	Included	Does not affect the UC solution

The PBUC is out of scope of this thesis since the thesis's aim is to consider the reliability and security of the system while PBUC is concerned about maximizing profit of selling energy. Therefore, the SCUC formulation will be used in this thesis.

3.5 Security-Constrained Unit Commitment (SCUC)

The goal of UC is to minimize the operating cost and satisfy load demand. However, when the security of the system is emphasized in the scheduled units, UC is called SCUC. SCUC is a UC method, which considers the power system security as a priority and hard constraint. Hence, the three main objectives of SCUC are satisfying load, ensuring security and minimizing operating cost. Satisfying load is a first priority and a hard constraint in the SCUC. Ensuring system security is achieved by providing ample reserve for supplying load in case of component outages. Lastly, minimizing cost is realized through inexpensive committed units and considering load satisfaction at the same time. SCUC is solved by ISO in order to plan the day-ahead unit schedule. ISO receives GENCOs' bids for each generation unit, and loads information from DISTCOs. The SCUC is solved to determine the schedule for the next day (24 hours) generating units at lowest operating cost while satisfying the system constraints. ISO also considers the transmission and voltage constraints in solving the SCUC since the transmission companies (TRANSCOs) submit the transmission grid information (i.e. the line availability and capability) to the ISO to assist in achieving transmission network security [35], [38].

In this thesis, SCUC is considered based on the mixed integer-linear programming (MILP) method to solve the microgrid scheduling problem. The microgrid SUCU modeling and its constraints are discussed in the next Chapter.

4 Chapter Four: SCUC Modeling for Microgrids

4.1 SCUC Constraints for Microgrids

The SCUC constraints in the microgrid are quite similar to the SCUC constraints in power systems or main grids. The difference is that the transmission constraints are not included in the SCUC in microgrids since there are no transmission lines in microgrids' networks. Instead of transmission constraints, microgrids have main power grid constraints controlling power flow from the main grid to the microgrids and vice versa. A novel constraint is also proposed in this thesis that could be added to control the change in power flow between main grid and microgrid on an hourly basis. Prevailing microgrid constraints are modeled, including load balance, generation limits, no-load/startup/shut down costs, ramp up/down limits and minimum up/down time limits. Each constraint is explained with its formulation as follows:

4.1.1 The load balance constraint.

The load balance constraint helps to ensure system balance between the load demand (D) and generation power (P). Wind power (W) is considered as negative load since it helps supply part of the load in addition to the microgrid generation units; In this work wind power generation is the only renewable energy considered to be integrated in microgrid as exhibited in Figure 4-1.

The main objective is to minimize total cost in (5), which is also call the objective equation. TC refers to total cost, P_{it} is the power of unit i at time t and C_i is the cost coefficient of unit i. PM_t represents the power flow from main grid and ρ_t is the market price of the main grid power. As there is no cost for wind power, it will not be added to the total cost. The load balance constraint is shown in (6), where the load balance is measured in hourly basis, D_t and W_t are the load demand and wind power at time t, respectively.

$$\boldsymbol{TC = \sum_i \sum_t C_i * P_{it} + \sum_t \rho_t * PM_t} \qquad (5)$$

$$\sum_i P_{it} + PM_t = D_t - W_t \qquad (6)$$

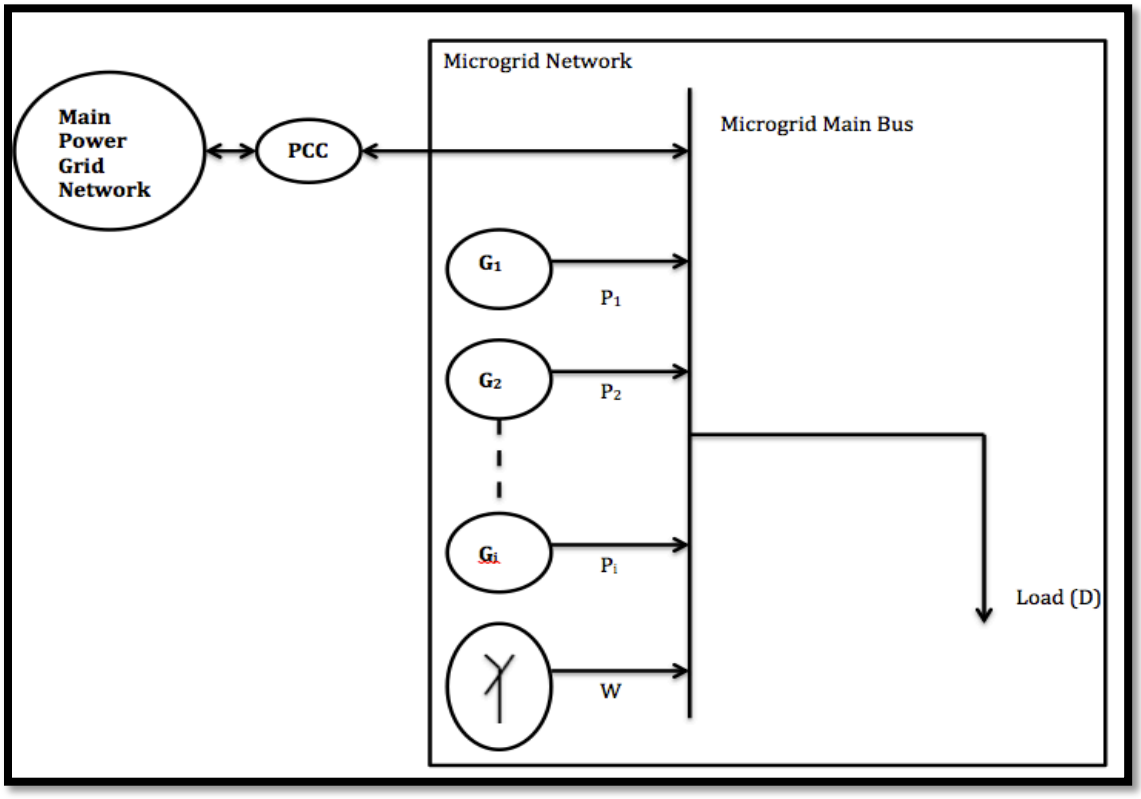

Figure 4-1: Simple structure of microgrid

Next, the objective equation (5) is revised depending on the constraints that are added to the SCUC problem.

4.1.2 Limits of generation units.

This constraint is to force the generation units to work within minimum and maximum limits. These limits are determined for each unit. Moreover, this constraint assists with network security and maintains the lifetime of each unit. In (7), the generation limit is considered for each unit. The objective equation will not change by adding the generation limits constraint.

$$P_i^{min} \leq P_{it} \leq P_i^{max} \qquad (7)$$

Where P_i^{min} represent the minimum generation limit for unit *i* whereas P_i^{max} referred to the maximum generation limit for unit *i*.

4.1.3 No load/start up/shut down indicators constraint.

This constraint helps system operators know the state of each unit. The commitment state (u_{it}) shows the ON/OFF state of the unit (when u_{it} equals 1, the unit is ON and when it equals 0 the unit is OFF). The startup indicator (y_{it}) represents the startup state. When the unit is started y_{it} is 1, otherwise it is 0. Similarly, the shut down indicator (z_{it}) indicates the switched off units as z_{it} equals 1 for these units right after shut down, otherwise it is 0. The constraint equations are displayed in (8) and (9).

$$u_{it} - u_{i,t-1} = y_{it} - z_{it} \qquad (8)$$

$$y_{it} + z_{it} \leq 1 \quad (9)$$

The generation limit constraint in (7) should be revised to have the commitment state indicator (u_{it}) as shown in (10).

$$P_i^{min} * u_{it} \leq P_{it} \leq P_i^{max} * u_{it} \quad (10)$$

4.1.4 No load cost.

No Load is a cost added only when the unit is committed (when the no load indicator u_{it} =1, the no load cost (nl_i) will be added to the unit *i*). It is also called labor cost. By considering the no load cost, objective equation in (5) is rewritten as shown in (11).

$$\boldsymbol{TC = \sum_i \sum_t C_i * P_{it} + \sum_t \rho_t * PM_t + \sum_i \sum_t nl_i * u_{it}} \quad (11)$$

4.1.5 Start up cost.

Start up cost (CST_i) is also called synchronization cost of the generator. The generator works with frequency of 60/50 Hz to synchronize with the power system. Accordingly, the turbine should rotate at a specific speed to make the generator frequency the same as the frequency of the system and synchronize the generator with the grid. This cost can be added only in the hour that the generator is first running on this process. Observing the startup indicator y_{it} (only when the y_{it} equals 1 meaning the unit just started), the startup cost should be added to the total cost. The startup cost can be added to the total cost as shown in (12).

$$\boldsymbol{TC} = \sum_i \sum_t \boldsymbol{C_i} * \boldsymbol{P_{it}} + \sum_t \boldsymbol{\rho_t} * \boldsymbol{PM_t} + \sum_i \sum_t \boldsymbol{nl_i} * \boldsymbol{u_{it}} + \sum_i \sum_t \boldsymbol{CST_i} * \boldsymbol{y_{it}} \quad (12)$$

4.1.6 Shut down cost.

Shut down cost (CSD_i) is also called the cooling down cost. Each unit has to be cooled down before the shut down process to maintain the lifetime of that unit. This cooling process has a cost that should be considered only when the unit is switched off. This cost should be added to the total cost only when the shut down indicator z_{it} equals 1, otherwise it should not be included. The objective equation in (12) is revised to include this cost as shown in (13), the final form of the objective in the SCUC model.

$$\boldsymbol{TC} = \sum_i \sum_t \boldsymbol{C_i} * \boldsymbol{P_{it}} + \sum_t \boldsymbol{\rho_t} * \boldsymbol{PM_t} + \sum_i \sum_t \boldsymbol{nl_i} * \boldsymbol{u_{it}} + \sum_i \sum_t \boldsymbol{CST_i} * \boldsymbol{y_{it}} + \sum_i \sum_t \boldsymbol{CSD_i} * \boldsymbol{z_i} \quad (13)$$

4.1.7 Reserve constraint.

The reserve (r_t) is an extra generation capacity in the system. This reserve must be determined such that it provides a sufficient capacity of power generation to supply the required load (D_t -W_t) in case of emergency. The reserve is measured depending on the system load as a percentage (α) of the total load as presented in (14) and (15). The committed units and the power flow from main grid should be able to supply the required load plus the reserve at any time. (16) represents the reserve constraint.

$$r_t = \alpha * (D_t - W_t) \quad (14)$$

$$R_t = D_t - W_t + r_t \quad (15)$$

$$PM_t + \sum_i P_i^{max} * u_{it} \geq R_t \quad (16)$$

4.1.8 Ramping up/down constraints.

Ramping constraint is added to SCUC to control any change in the unit generation across two consecutive hours. The ramp up (RU_i) constraint is the maximum power generation rate that can be added in unit generation in one hour compared to the same unit generation across the previous hour. On the other hand, the ramp down rate (RD_i) is the maximum drop rate in unit generation across two consecutive hours.

These constraints can be modeled in the SCUC model as shown in (17) for ramping up and in (18) for ramping down.

$$P_{it} - P_{i,t-1} \leq RU_i \quad (17)$$

$$P_{i,t-1} - P_{it} \leq RD_i \quad (18)$$

4.1.9 Minimum up/down time constraints.

Minimum up time (MU_i) is the minimum time that the unit stays ON when it is turned ON or committed. The minimum down time (MD_i) is the minimum time considered for the unit when it is turned OFF before it is turned ON again. These constraints are for the cooling down and synchronization processes.

In order to accurately count the up time of a unit, the duration from first commit of the unit must be modeled. The time counter (su_{it}) is modeled as in (19) and (20).

$$0 \leq su_{it} \leq MN * u_{it} \quad (19)$$

$$(MN + 1) * u_{it} - MN \leq su_{it} - su_{i,t-1} \leq 1 \qquad (20)$$

Where *MN* is the maximum number of hours that the unit can be ON.

Similarly, the time counter of down duration (sd_{it}) is calculated by (21) and (22).

$$0 \leq sd_{it} \leq MF * (1 - u_{it}) \qquad (21)$$

$$1 - (MF + 1) * u_{it} \leq sd_{it} - sd_{i,t-1} \leq 1 \qquad (22)$$

Where *MF* is the maximum number of possible down hours. With the number of hours that the unit is up or down, the minimum time up/down constraints are modeled as shown in (23) and (24), respectively.

$$su_{it} \geq MU_i * z_{i,t+1} \qquad (23)$$

$$sd_{it} \geq MD_i * y_{i,t+1} \qquad (24)$$

The time counter (*su*) should reach the minimum up time for the unit, and it is acceptable if it stays ON for additional time. Likewise, the down time counter (*sd*) must reach the minimum down time of the unit. Also it is possible that the unit stays OFF for additional time.

4.1.10 Main power flow constraint.

The transmission line connecting the main grid and the microgrid has a maximum capacity (PM^{max}) for power transfer from and to the microgrid. This constraint controls the flow of power from main grid to microgrid and vice versa. By adding this constraint, the security of the line that joins the microgrid with utility network is enhanced. The formulation of this constraint is presented in (25).

$$-PM^{max} * OS_t \leq PM_t \leq PM^{max} * OS_t \qquad (25)$$

Where OS_t is the operation state of the microgrid at time t, if it is grid connected, the OS_t equals 1, otherwise it is zero. When the value of PM_t is a positive value, the microgrid consumes power from the main grid. On the contrary, if it is negative, the microgrid delivers power to the main grid.

4.1.11 Main power flow fluctuation constraint.

In this thesis, wind power is integrated in the microgrid. The nature of wind may cause a fluctuation in wind power generation. As a result, the main grid may suffer from the wind power fluctuation as this fluctuation harms the main grid power system and affects the main power system units. This is a novel constraint that is proposed to limit the fluctuation in the main grid power system. Utility companies have to select a way of adding this constraint. Following are two ways of applying this new constraint:

1. By forcing it on all microgrids in its distribution network, specifying the maximum limit of drop or increase in the main power flow from and to the microgrid between two consecutive hours.
2. By selecting specific microgrids with a harmful wind power fluctuation and reimbursing them the lost revenue in order to reduce the wind power fluctuation. Utility can be part of the microgrid only for the lost revenue caused by limiting the fluctuation instead of building an extra unit to solve the fluctuation. These projects may be more expensive than paying the lost revenue to the microgrids.

In this thesis, option one is considered in order to keep simple

calculations since the purpose is to see the impact of adding this constraint in the SCUC problem. Thus, this constraint is just enforced by the utility to all microgrids in the main grid network and is termed Utility Grid Code (UGC). UGC is a code that determines the drop or increase in power transfer (Δ_{UGC}) across two consecutive hours in the main power flow *PM*. Hence, this constraint can be modeled as shown in (26).

$$|PM_t - PM_{t-1}| \leq \Delta_{UGC} \tag{26}$$

5 Chapter Five: Numerical Analysis

5.1 Wind Forecasting Models

The wind forecasting models used in this thesis are ARIMA and ANN. Forecasting considered is short-term (24-hour forecasting) since the goal of this study is microgrid operation. A comparison between these two models demonstrates that the ANN model outperforms the ARIMA model. Model accuracy is measured by using mean absolute percentage error (MAPE). The formula of MAPE is shown in (27).

$$MAPE = \frac{1}{N}\sum_{i=1}^{N}\left|\frac{A(i)-F(i)}{A(i)}\right| * 100\% \qquad (27)$$

where the *A(i)* is the actual value and the *F(i)* is the forecasted one. *N* represents the number of steps in the time series [39].

5.1.1 Preparing data for forecasting models.

Wind power historical data was gathered from the National Renewable Energy Laboratory (NREL) website [40]. The location of the wind turbine, from which the data is obtained, is near the Rocky Mountains. This data represents power production in MW and are ten-minute step data across one year. For these cases, only one-day historical data is selected as input for the models to forecast next day wind power production. The data has been normalized to improve quality before using in the forecasting models.

5.1.2 ARIMA model.

Autoregressive integrated moving average (ARIMA) is used to forecast one-day ahead wind power generation. By using (2), the ARIMA model has been tested on different (p, d, q) orders as shown in Table 5-1.

Table 5-1: MAPE for different p and q orders

ARIMA (p, 0, q)	MAPE
ARIMA (1,0,0)	18.41%
ARIMA (1, 0,1)	43.57%
ARIMA (2, 0,0)	11.75%
ARIMA (2, 0,1)	28.74%
ARIMA (2, 0,2)	25.60%
ARIMA (3, 0,0)	13.49%
ARIMA (3, 0,1)	15.78%
ARIMA (3, 0,2)	100.38%
ARIMA (3, 0,3)	98.03%
ARIMA (4, 0,0)	13.45%
ARIMA (4, 0,1)	65.39%
ARIMA (4, 0,2)	102.33%
ARIMA (4, 0,3)	105.17%
ARIMA (4, 0,4)	99.15%
ARIMA (5, 0,0)	13.70%
ARIMA (5, 0,1)	57.22%
ARIMA (5, 0,2)	104.24%
ARIMA (5, 0,3)	119.31%
ARIMA (5, 0,4)	91.55%
ARIMA (5, 0,5)	107.79%
ARIMA (6, 0,0)	13.82%
ARIMA (7, 0,0)	13.86%
ARIMA (8, 0,0)	13.87%
ARIMA (9, 0,0)	13.85%
ARIMA (10,0,0)	13.83%

Table 5-2: The AR (2) coefficients

The 1st AR coefficient	1.778
The 2nd AR coefficient	-0.788

Table 5-1, demonstrates that configurations which include only the autoregressive part produce the best results for MAPE. Hence, this data is an autoregressive time series data. The smallest MAPE means the higher accuracy for the forecasted wind power. The smallest MAPE is about 11.75% and it is achieved by the ARIMA (2,0,0), which is also known as AR (2). Figure 5-1 shows the actual and forecasted wind power generation for one-day. The AR and MA coefficients are determined by employing a Matlab function (armax) to help our data fit the ARIMA model. The AR coefficients for the AR (2) are shown in Table 5-2.

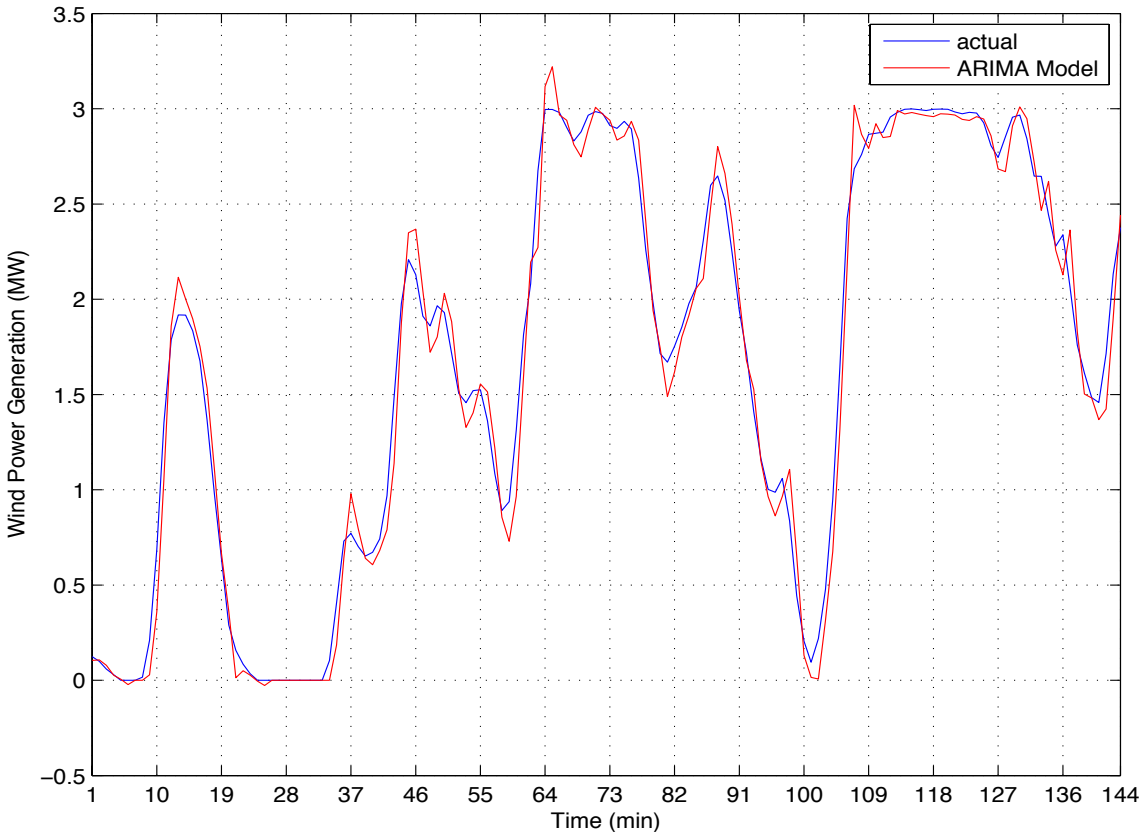

Figure 5-1: The actual and forecasted wind power based on ARIMA (2, 0, 0)

5.1.3 ANN model.

Artificial neural network is the recommended forecasting method for renewable energy as it provides more accurate results compared to other methods. Many power utilities use the ANN method for short-term forecasting. As a result, ANN is selected to compare results with ARIMA. In ANN, it is necessary to select three main parameters as following: number of input vectors, number of hidden layers and the number of output vectors. The input used is one-day wind power historical data as one vector input. Also, the output vector is one vector, which is the forecasted wind power data. ANN is modeled by the NN toolbox in Matlab as shown in Figure 5-2. The time series application has been selected since our historical data is a time based series.

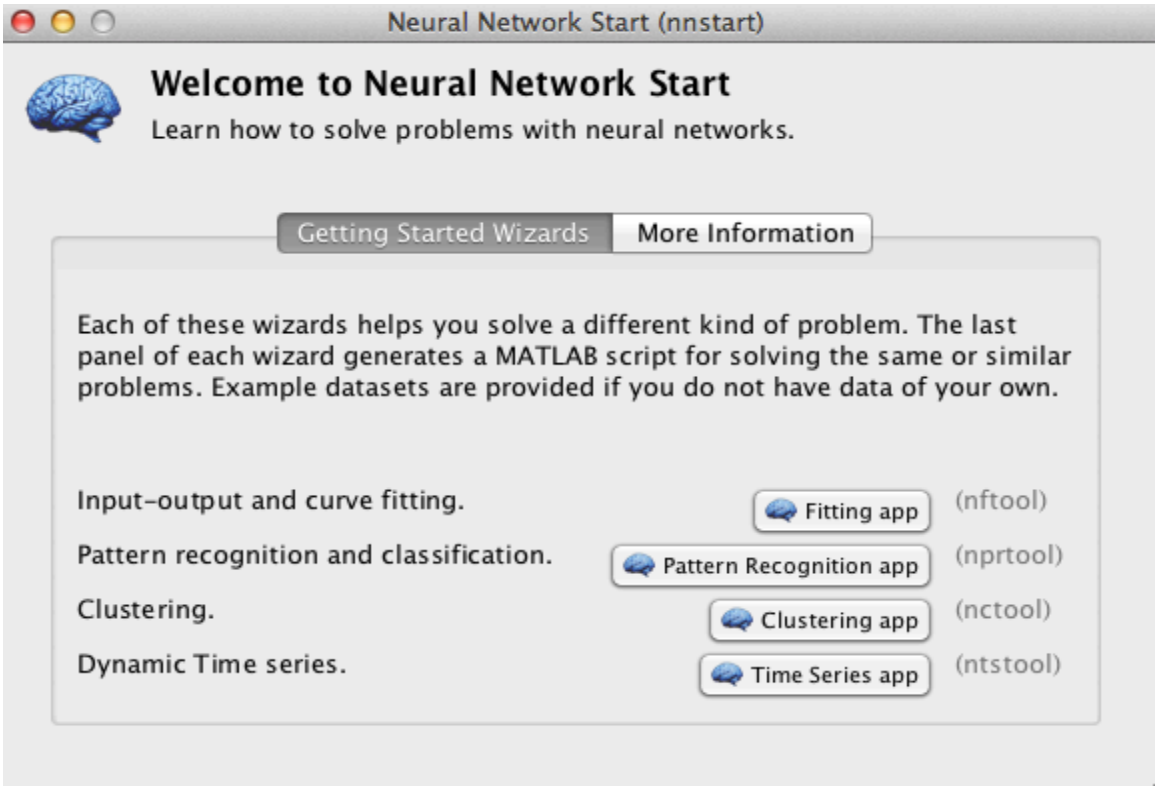

Figure 5-2: NN toolbox start

The time series model is divided into three types depending on the model input. These types are nonlinear autoregressive with external input (NARX), nonlinear autoregressive (NAR) and nonlinear input-output. Since the input is external as it is one-day historical data, NARX model has been considered. Figure 5-3 shows the difference between these three types.

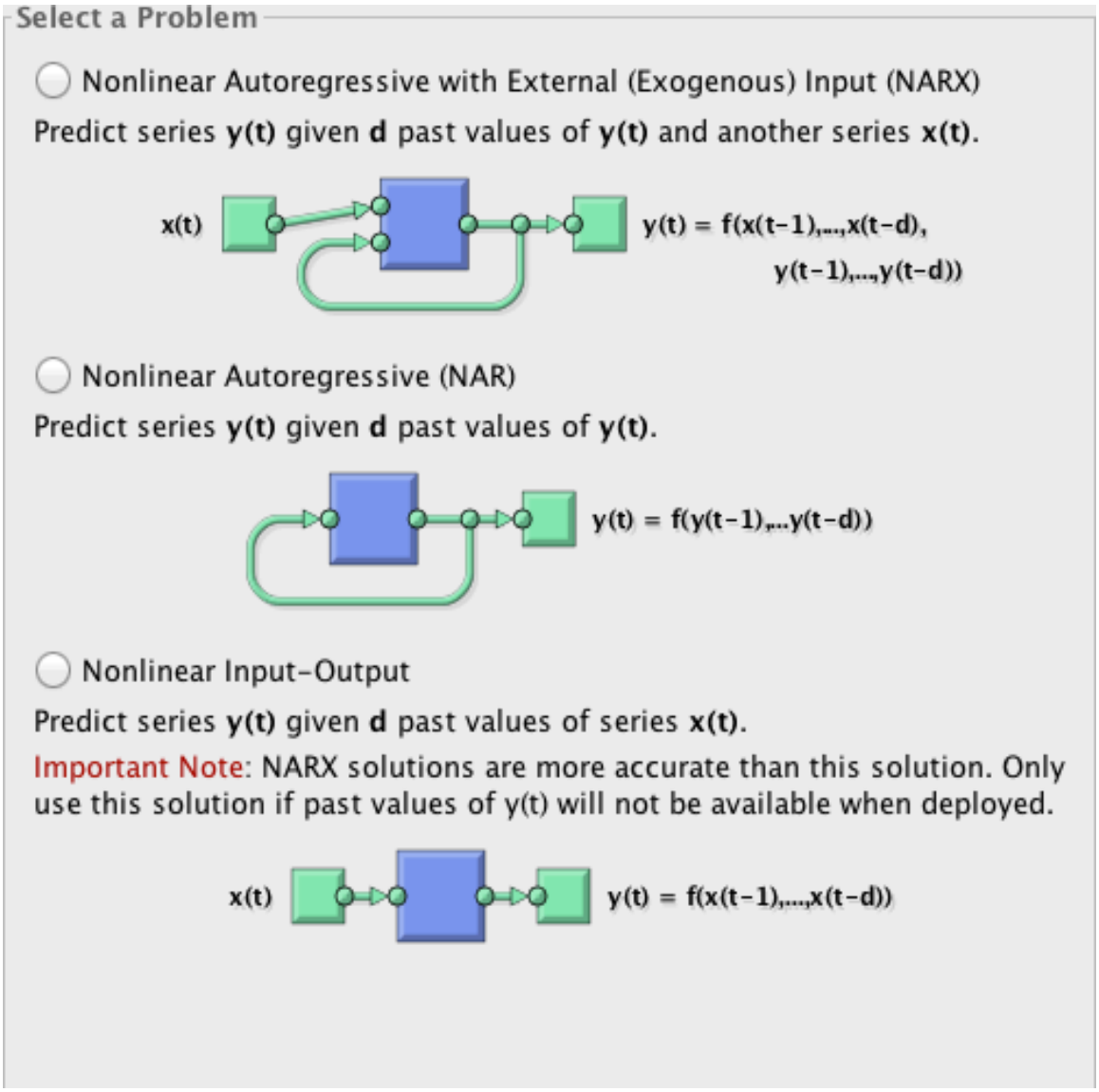

Figure 5-3: Kinds of nonlinear time series problem

After determining the time series problem, the input and target vectors are entered in the model. A 15% of the target data must be reserved for testing and validating the model. Next, the time delay and the hidden layers are selected. Applying a selected training algorithm (Levenberg-Marqurdt, Figure 5-4), the data will be trained until desired accuracy is achieved. If the forecasting error is not satisfactory, the data will train again after changing the model parameters such as time delay, hidden layers or the training algorithm. The time delay is selected to be 1 for all cases and the model is executed for different hidden layers as displayed in Table 5-3 with the MAPE results for each case.

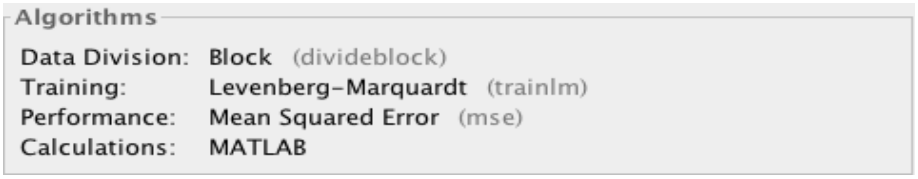

Figure 5-4: The training algorithm

Table 5-3: The MAPE for ANN with different hidden layers

The number of hidden layers	MAPE
30	14.83%
25	12.20%
20	10.81%
15	9.02%
10	8.33%
5	6.95%
3	5.59%
1	4.60%

Form Table 5-3, it is clear that when the number of hidden layers decreases, the MAPE is decreased. This process demonstrates that the best and smallest MAPE is 4.6% when there is only one hidden layer in the ANN model. Therefore, the selected ANN

model has only one input vector, one hidden layer and one output vector as shown in Figure 5-5.

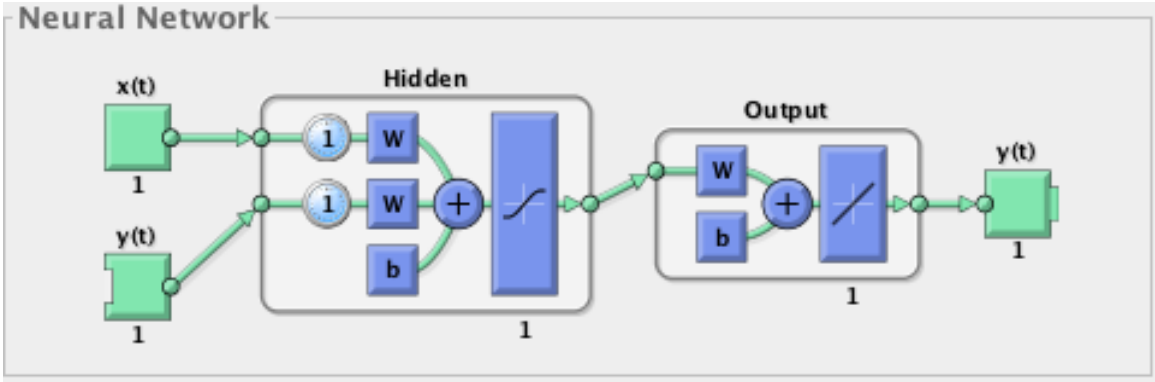

Figure 5-5: ANN model

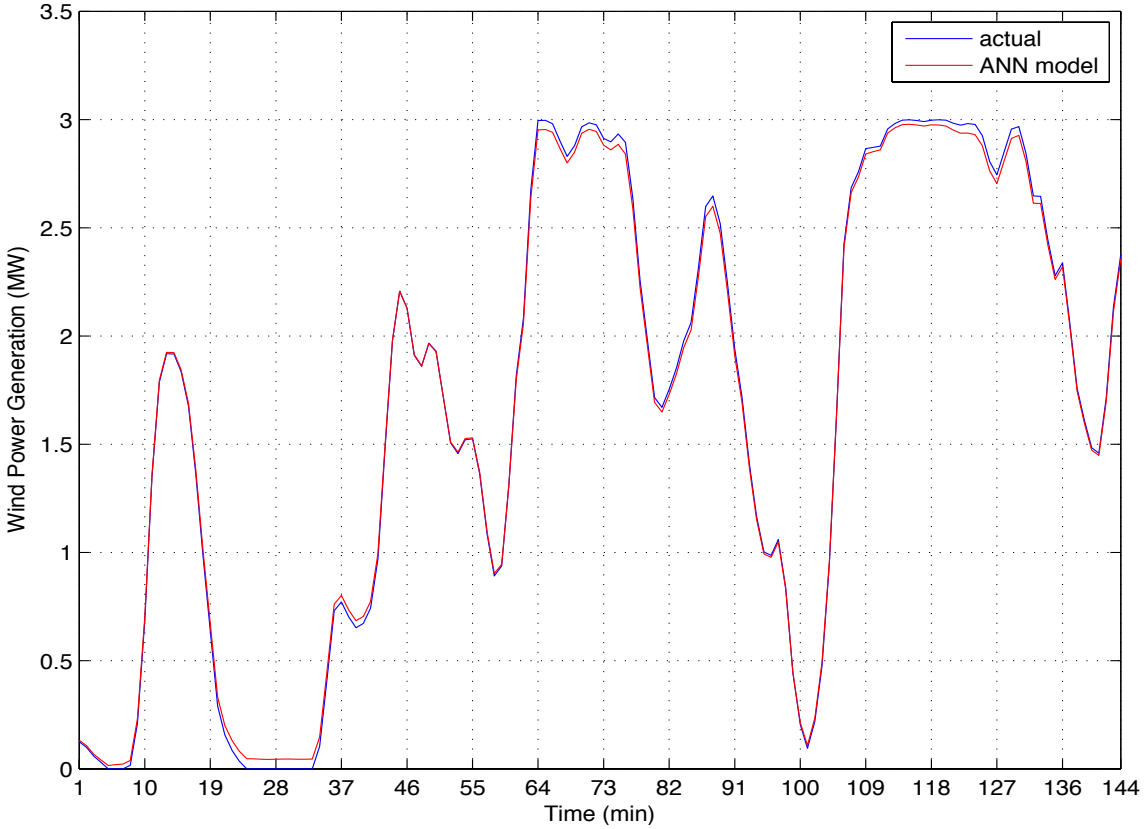

Figure 5-6: The actual and forecasted wind power data with ANN model

Figure 5-6 shows the actual and forecasted wind power generation by using ANN model. By comparing the result with the ARIMA model, it can be seen that the ANN model outperforms the ARIMA model by reducing the MAPE from 11.75% to 4.60%.

The forecasted wind power generation is close to the actual wind power generation when ANN model is used but is not very accurate when ARIMA model is used as demonstrated in Figure 5-7 for both models together. This result supports the recommendation of using ANN model for short-term forecasting.

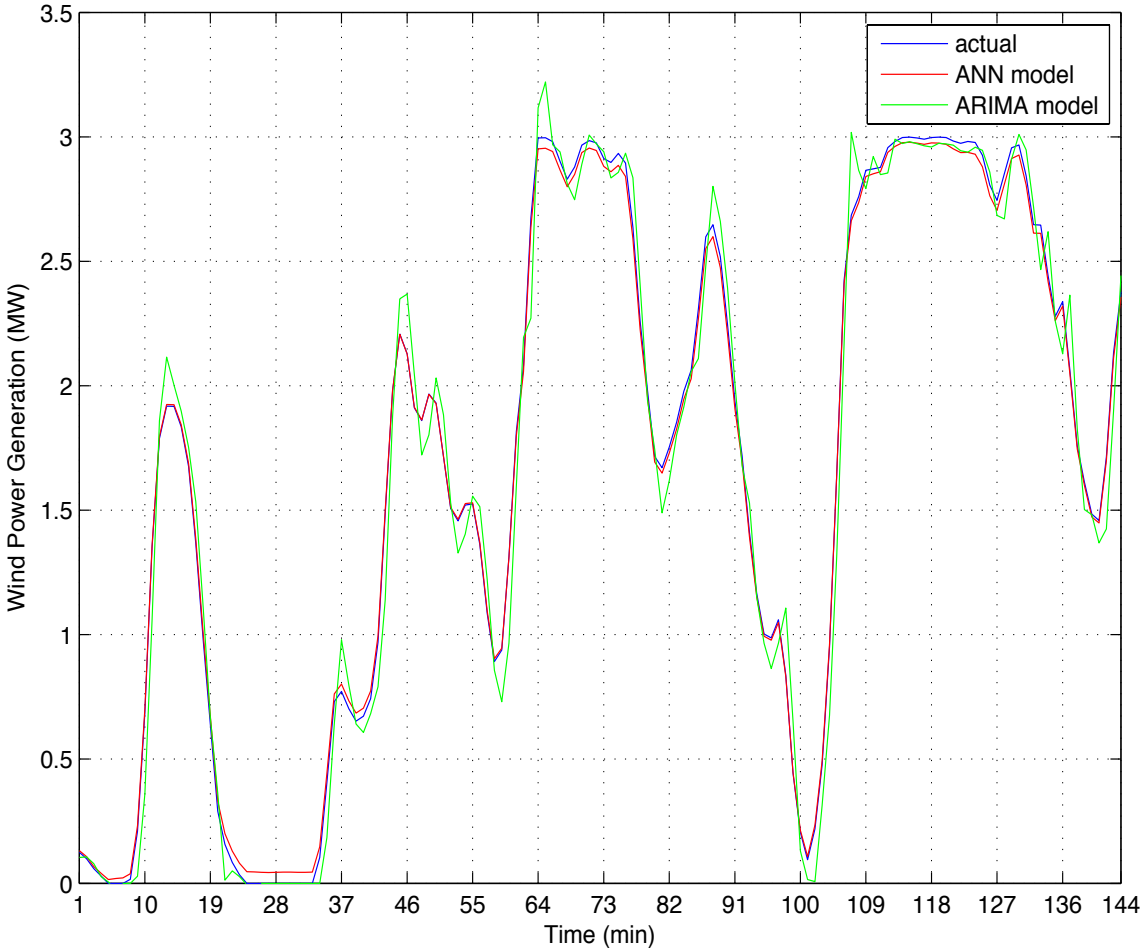

Figure 5-7: Comparison between ANN and ARIMA models with actual data

The data used in above models are considered to be associated with a 3MW wind turbine. The data can be scaled up to 4MW and 5MW to be used in different cases for SCUC problems and further showing the impact of increase of the penetration of wind power in microgrids.

5.2 SCUC Model

The considered SCUC constraints in this case study are load balance, generation limit, ramping up/down, minimum up/down, main power flow and the novel constraint for controlling the main power fluctuation.

5.2.1 Preparing data for SCUC model.

The microgrid dispatchable generation capacity is considered to be 16MW with four generators and one wind turbine (its capacity is 3MW, 4MW or 5MW depending on the case as described below). The microgrid is connected to the main grid via a distribution line with a 10 MW capacity. The data of generators, hourly load and the main power market price are gathered from [17] and shown in Tables 5-4, 5-5, 5-6, respectively. .

Table 5-4: Generators data

Unit	Min. Power (MW)	Max. Power (MW)	Cost coefficient ($/MWh)	Ramping up/down (MW/h)	Minimum up/down (h)
G_1	1	5	27.7	2.5	3
G_2	1	5	39.1	2.5	3
G_3	0.8	3	61.3	3	1
G_4	0.8	3	65.6	3	1

Table 5-5: The hourly load data

Hour	**1**	**2**	**3**	**4**	**5**	**6**	**7**	**8**
Load (MW)	8.73	8.54	8.47	9.03	8.79	8.81	10.12	10.93
Hour	**9**	**10**	**11**	**12**	**13**	**14**	**15**	**16**
Load (MW)	11.19	11.78	12.08	12.13	13.92	15.27	15.36	15.69
Hour	**17**	**18**	**19**	**20**	**21**	**22**	**23**	**24**
Load (MW)	16.13	16.14	15.56	15.51	14.00	13.03	9.82	9.45

Table 5-6: The hourly main power market price data

Hour	**1**	**2**	**3**	**4**	**5**	**6**	**7**	**8**
Price($/MWh)	15.03	10.97	13.51	15.36	18.51	21.8	17.3	22.83
Hour	**9**	**10**	**11**	**12**	**13**	**14**	**15**	**16**
Price($/MWh)	21.84	27.09	37.06	68.95	65.79	66.57	65.44	79.79
Hour	**17**	**18**	**19**	**20**	**21**	**22**	**23**	**24**
Price($/MWh)	115.45	110.28	96.05	90.53	77.38	70.95	59.42	56.68

Table 5-7: Actual and forecasted hourly wind data for 3MW, 4MW and 5MW wind turbine

Hour	3-MW wind turbine			4-MW wind turbine			5-MW wind turbine		
	actual	ANN	ARIMA	actual	ANN	ARIMA	actual	ANN	ARIMA
1	0.0520	0.0847	0.0633	0.0694	0.1129	0.0844	0.0867	0.1411	0.1055
2	0.6750	0.6931	0.4507	0.9000	0.9241	0.6009	1.1250	1.1551	0.7512
3	1.6151	1.6106	1.7210	2.1534	2.1475	2.2947	2.6918	2.6844	2.8683
4	0.2006	0.2299	0.2788	0.2674	0.3065	0.3717	0.3343	0.3831	0.4647
5	0.0000	0.0339	-0.0020	0.0000	0.0452	-0.0027	0.0000	0.0565	-0.0033
6	0.2067	0.2358	0.1076	0.2756	0.3144	0.1435	0.3445	0.393	0.1793
7	0.7513	0.7678	0.7194	1.0017	1.0238	0.9592	1.2521	1.2797	1.1990
8	1.9284	1.9160	1.8191	2.5712	2.5547	2.4255	3.2140	3.1934	3.0318
9	1.6823	1.6763	1.6826	2.2430	2.2350	2.2435	2.8038	2.7938	2.8043
10	1.1855	1.1918	1.1686	1.5807	1.5890	1.5581	1.9759	1.9863	1.9477
11	2.5907	2.5596	2.3958	3.4543	3.4128	3.1944	4.3179	4.266	3.9930
12	2.9228	2.8823	2.8735	3.8971	3.8430	3.8313	4.8714	4.8038	4.7892
13	2.7554	2.7197	2.8054	3.6738	3.6263	3.7405	4.5923	4.5329	4.6757
14	1.8251	1.8155	1.7941	2.4335	2.4207	2.3921	3.0419	3.0259	2.9902
15	2.3966	2.3715	2.3515	3.1954	3.1620	3.1353	3.9943	3.9525	3.9192

16	1.3703	1.3719	1.4635	1.8270	1.8292	1.9513	2.2838	2.2865	2.4392
17	0.4763	0.4992	0.5404	0.6351	0.6656	0.7205	0.7939	0.832	0.9007
18	1.8227	1.8119	1.5290	2.4303	2.4159	2.0387	3.0379	3.0199	2.5483
19	2.9246	2.8840	2.8538	3.8994	3.8453	3.8051	4.8743	4.8066	4.7563
20	2.9962	2.9533	2.9465	3.9949	3.9377	3.9287	4.9936	4.9221	4.9108
21	2.9412	2.9000	2.9185	3.9216	3.8667	3.8913	4.9020	4.8334	4.8642
22	2.8349	2.7971	2.8081	3.7799	3.7294	3.7441	4.7249	4.6618	4.6802
23	2.2544	2.2333	2.3156	3.0059	2.9777	3.0875	3.7574	3.7221	3.8593
24	1.7963	1.7872	1.6687	2.3950	2.3830	2.2249	2.9938	2.9787	2.7812

Wind data is changed from 10-minute step to hourly step by taking the average value for each hour. That is because SCUC is normally solved for one-day ahead in an hourly basis. Also, wind data is scaled up to 4MW and 5MW for solving the SCUC and observe the impact of increase of the wind penetration in the microgrids. Table 5-7 exhibits the wind data (actual and forecasted) when the wind turbine capacity is 3MW, 4MW and 5MW.

5.2.2 SCUC cases.

Two SCUC cases are considered for the above-mentioned microgrid as following:

- **Case 1**: Before adding the main power fluctuation constraint.
- **Case 2**: After adding the main power fluctuation constraint.

For Case 1, there are three sub-cases as follows:

- Case 1-1: SCUC with actual and forecasted wind power data when using a 3MW-wind turbine.
- Case 1-2: SCUC with actual and forecasted wind power data when using a 4MW-wind turbine.

- Case 1-3: SCUC with actual and forecasted wind power data when using a 5MW-wind turbine.

For Case 2, only actual wind data is used to show the effect of adding the main power fluctuation constraint. Also, there are three sub-cases as following:

- Case 2-1: Controlling the main power fluctuation when using a 3MW-wind turbine.
- Case 2-2: Controlling the main power fluctuation when using a 4MW-wind turbine.
- Case 2-3: Controlling the main power fluctuation when using a 5MW-wind turbine.

5.2.2.1 Case 1.

Case 1-1: The SCUC is solved for the microgrid that has a 3MW wind turbine integrated in its network. Table 5-8 shows the results of total cost for actual data, ANN forecasted model and ARIMA forecasted model. From Table 5-8, it is clear that ANN forecasting model is more accurate than ARIMA model in the total operating cost. ANN provides a more accurate total operating cost than ARIMA, comparing to the actual case.

Table 5-8: The total one-day operating cost for microgrid with a 3MW-wind turbine

Actual	Forecast (ARIMA)	Forecast (ANN)
$7267.204	$7321.012	$7287.238
ERROR (%)	($0.74)	($0.28)

Table 5-9: The committed state for the units with actual, ANN forecast and ARIMA forecast

H	Actual case				ANN forecast				ARIMA forecast			
	G_1	G_2	G_3	G_4	G_1	G_2	G_3	G_4	G_1	G_2	G_3	G_4
1	0	0	0	0	0	0	0	0	0	0	0	0
2	0	0	0	0	0	0	0	0	0	0	0	0
3	0	0	0	0	0	0	0	0	0	0	0	0
4	0	0	0	0	0	0	0	0	0	0	0	0
5	0	0	0	0	0	0	0	0	0	0	0	0
6	0	0	0	0	0	0	0	0	0	0	0	0
7	0	0	0	0	0	0	0	0	0	0	0	0
8	0	0	0	0	0	0	0	0	0	0	0	0
9	0	0	0	0	0	0	0	0	0	0	0	0
10	1	0	0	0	1	0	0	0	1	0	0	0
11	1	1	0	0	1	1	0	0	1	1	0	0
12	1	1	1	1	1	1	1	1	1	1	1	1
13	1	1	1	1	1	1	1	1	1	1	1	1
14	1	1	1	1	1	1	1	1	1	1	1	1
15	1	1	1	0	1	1	1	0	1	1	1	0
16	1	1	1	1	1	1	1	1	1	1	1	1
17	1	1	1	1	1	1	1	1	1	1	1	1
18	1	1	1	1	1	1	1	1	1	1	1	1
19	1	1	1	1	1	1	1	1	1	1	1	1
20	1	1	1	1	1	1	1	1	1	1	1	1
21	1	1	1	1	1	1	1	1	1	1	1	1
22	1	1	1	1	1	1	1	1	1	1	1	1
23	1	1	0	0	1	1	0	0	1	1	0	0
24	1	1	0	0	1	1	0	0	1	1	0	0

Table 5-10: The units generation (MW) with actual, ANN forecast and ARIMA forecast cases

H	Actual case				ANN forecast				ARIMA forecast			
	G_1	G_2	G_3	G_4	G_1	G_2	G_3	G_4	G_1	G_2	G_3	G_4
1	0	0	0	0	0	0	0	0	0	0	0	0
2	0	0	0	0	0	0	0	0	0	0	0	0
3	0	0	0	0	0	0	0	0	0	0	0	0

4	0	0	0	0	0	0	0	0	0	0	0	0
5	0	0	0	0	0	0	0	0	0	0	0	0
6	0	0	0	0	0	0	0	0	0	0	0	0
7	0	0	0	0	0	0	0	0	0	0	0	0
8	0	0	0	0	0	0	0	0	0	0	0	0
9	0	0	0	0	0	0	0	0	0	0	0	0
10	2.5	0	0	0	2.5	0	0	0	2.5	0	0	0
11	5	2.5	0	0	5	2.5	0	0	5	2.5	0	0
12	5	5	3	3	5	5	3	3	5	5	3	3
13	5	5	3	3	5	5	3	3	5	5	3	3
14	5	5	3	3	5	5	3	3	5	5	3	3
15	5	5	3	0	5	5	3	0	5	5	3	0
16	5	5	3	3	5	5	3	3	5	5	3	3
17	5	5	3	3	5	5	3	3	5	5	3	3
18	5	5	3	3	5	5	3	3	5	5	3	3
19	5	5	3	3	5	5	3	3	5	5	3	3
20	5	5	3	3	5	5	3	3	5	5	3	3
21	5	5	3	3	5	5	3	3	5	5	3	3
22	5	5	3	3	5	5	3	3	5	5	3	3
23	5	5	0	0	5	5	0	0	5	5	0	0
24	5	5	0	0	5	5	0	0	5	5	0	0

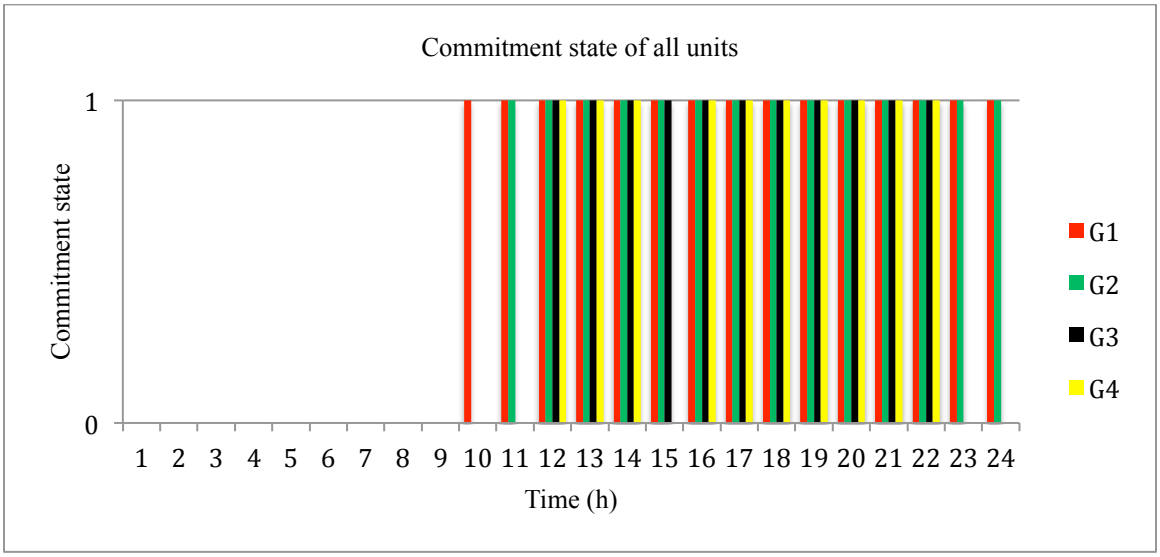

Figure 5-8: The commitment state of all units over 24 hours

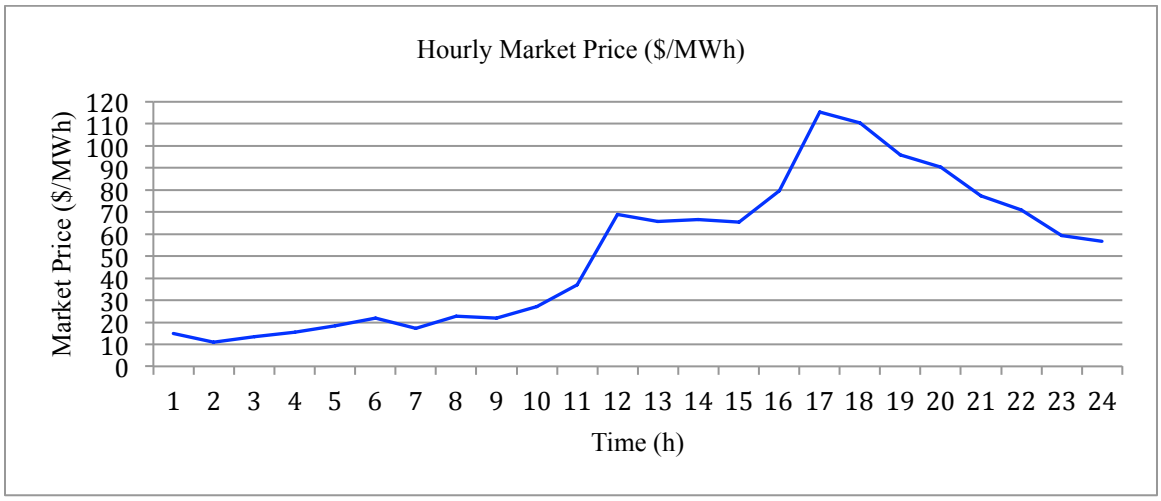

Figure 5-9: The market price of the main grid power over 24 hours

Tables 5-9 and 5-10 show the commitment state and the generation for each unit in all cases. It is obvious from the above tables that forecasting error does not impact the commitment state or the generation of the units. These are affected by the market price and the cost coefficient of the units. Figures 5-8 and 5-9 show that the first nine hours when the units are OFF (commitment state is 0) and the main grid supplies the load since the market price for these hours is less than the cost coefficient of all units. As a result, it is cheaper to supply the load from the main grid. Then the units 1 and 2 are turned on at hours 10 and 11 since the cost coefficient for them is cheaper than the market price. When the market price goes higher than the cost coefficient (like in hours 12, 13 and 14), all units are started up (commitment state is 1) at full capacity since the extra generation can be sold back to the utility and considered as microgrid saving. At hour 15, the market price is dropped down the cost coefficient for the unit 4, so it is not an economic decision to leave it working, especially when the minimum up time is reached. Similarly in hours 23 and 24, the cost coefficient for units 3 and 4 is higher than that market price, so it

is better to turn these units OFF since they cost more than main grid power. Figure 5-10 shows the power flow to and from the microgrid for actual case, ANN forecast and ARIMA forecast cases. It is presented that the power supply from the main grid dropped suddenly between hours 10 and 12 due to a sudden rise in the market price of the main grid power.

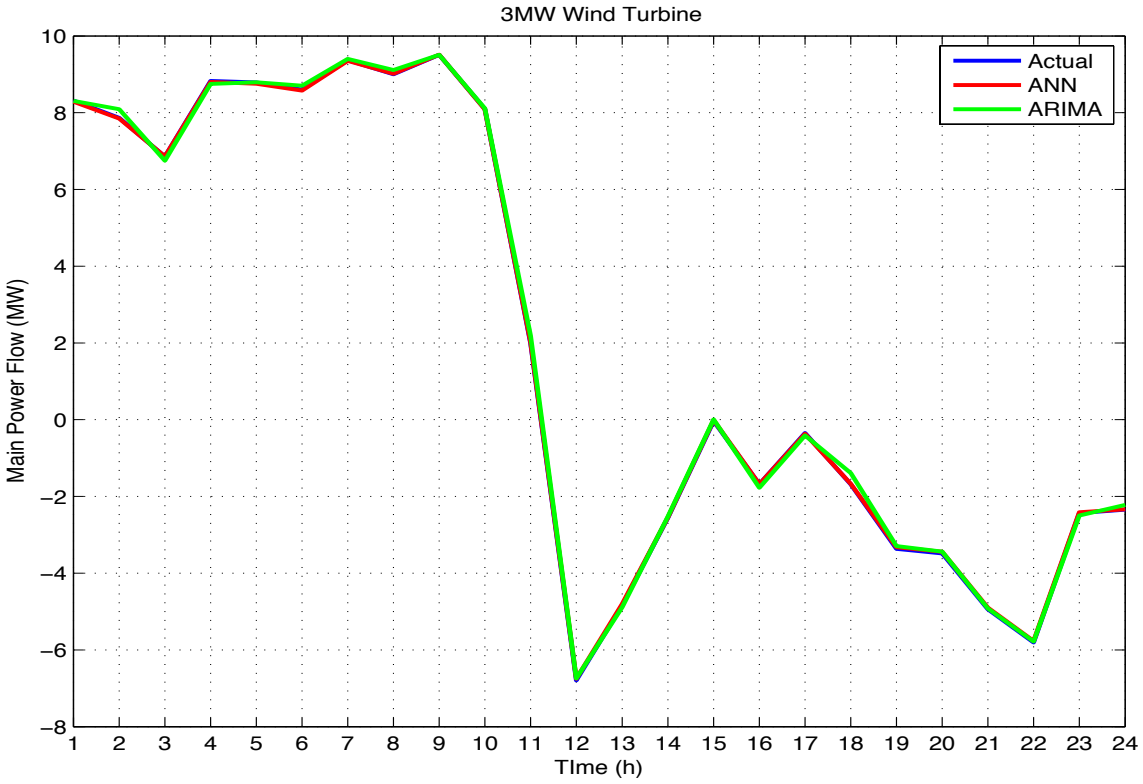

Figure 5-10: The main power flow (3MW-wind turbine)

Case 1-2: The wind turbine capacity is scaled up to 4MW in order to observe the impact of increase of wind power penetration in the microgrid. The commitment state and the generation of units are exactly the same as the previous case (Tables 5-9 and 5-10). The only noticeable change in this case is that the total operating cost is decreased. Hence, the total operating cost of the microgrid will be decreased if wind

penetration in microgrid is increased. Similarly, the ANN forecasting model provides more accurate results for operating cost as shown in Table 5-11. Also, the main power flow has dropped suddenly as in previous case, Figure 5-11.

Table 5-11: The total one-day operating cost for microgrid with a 4MW-wind turbine

Actual	Forecast (ARIMA)	Forecast (ANN)
$6433.014	$6504.757	$6459.721
ERROR (%)	($1.12)	($0.42)

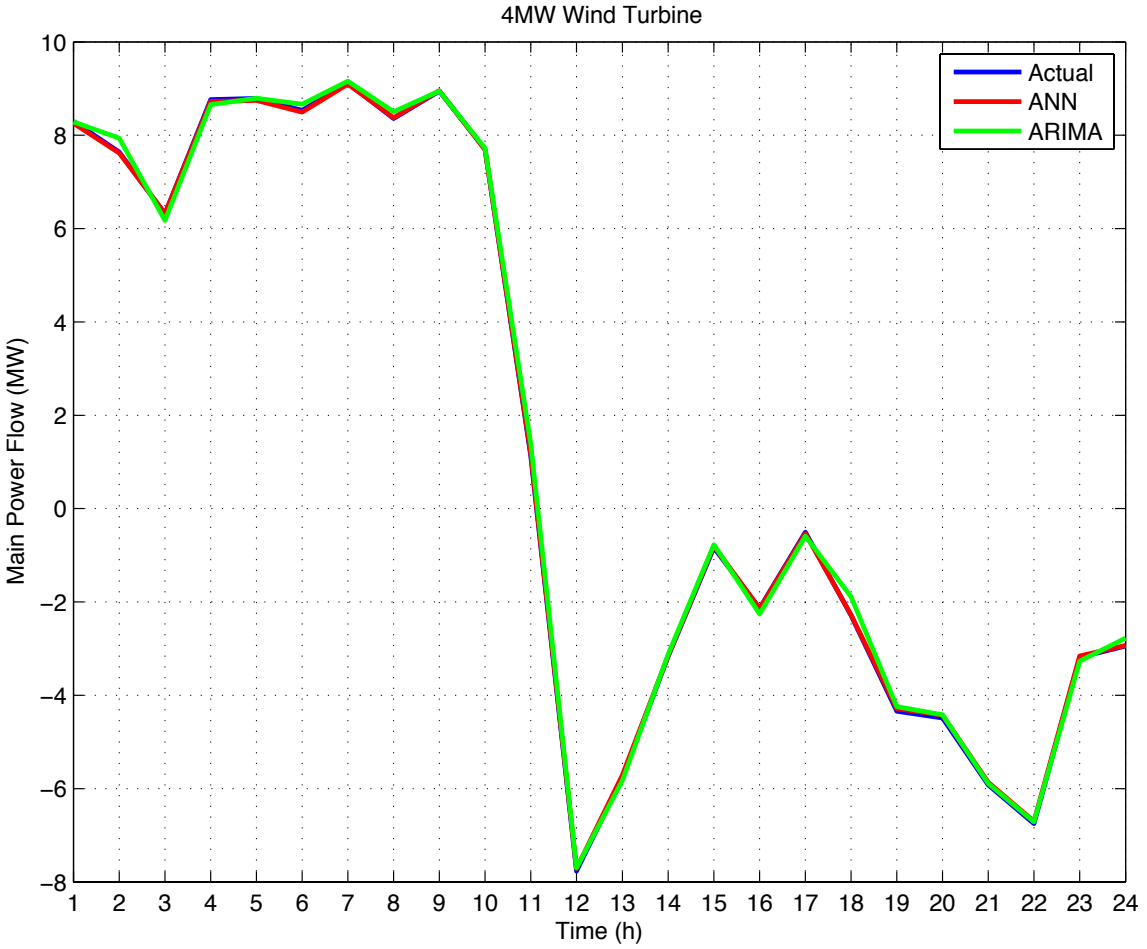

Figure 5-11: The main power flow (4MW-wind turbine)

Case 1-3: Wind turbine capacity is scaled up to 5MW. The results for this case do not have a significant deviation from the previous cases. The total operating cost

decreased when the wind turbine capacity is increased, Table 5-12. Likewise, the ANN model outperformed the ARIMA model by providing closer results to the actual case. The main power flow still has a dangerous fluctuation between hours 10 and 12, Figure 5-12.

Table 5-12: The total one-day operating cost for microgrid with a 5MW-wind turbine

Actual	Forecast (ARIMA)	Forecast (ANN)
$5598.785	$5688.472	$5632.192
ERROR (%)	($1.60)	($0.60)

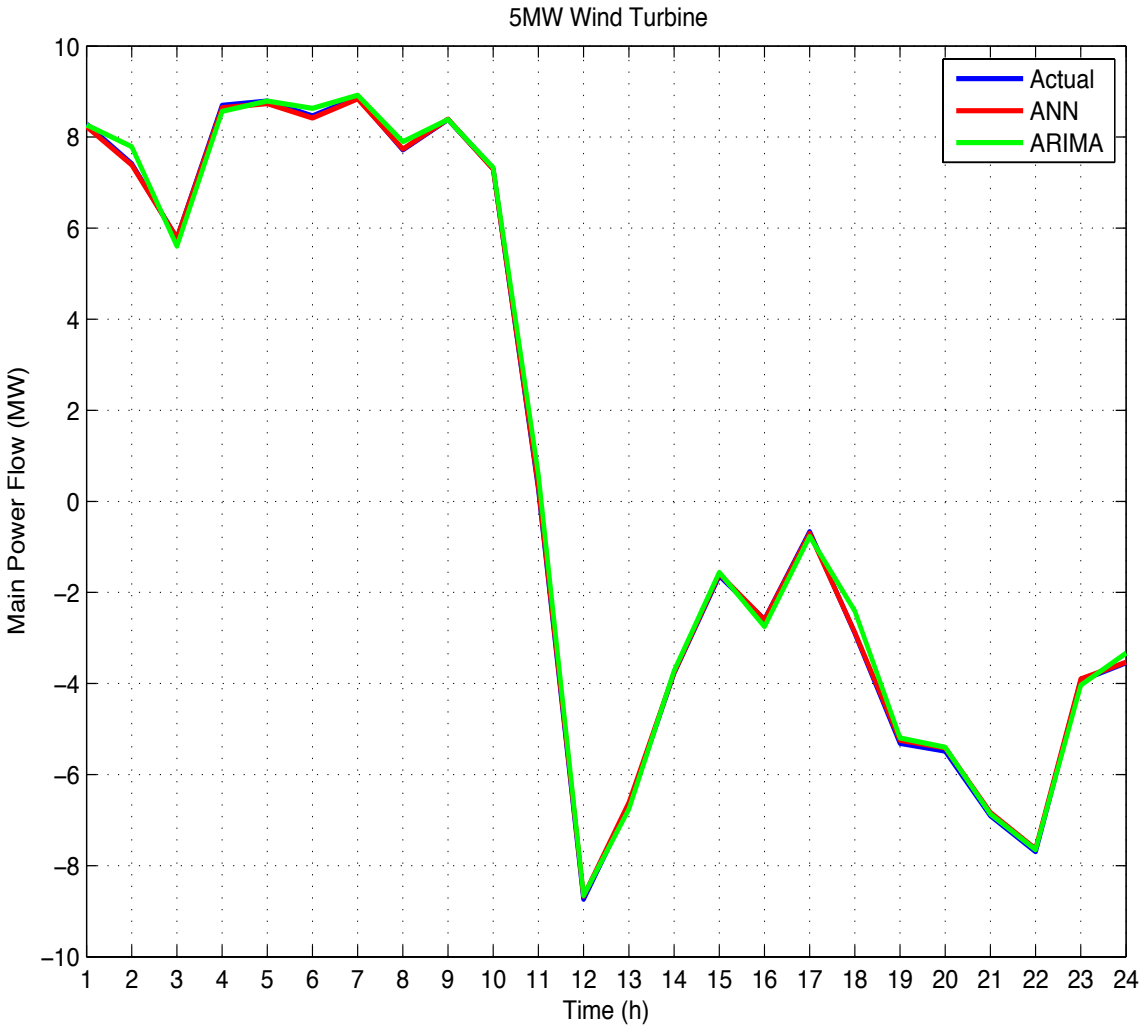

Figure 5-12: The main power flow (5MW-wind turbine)

It is observed from previous cases that the change in the main power market price and the cost coefficient of the microgrid units may cause a fluctuation. This fluctuation would harm the main grid power system. Consequently, a new constraint is proposed for the main grid operator to avoid this fluctuation. The utilities can impose it to the microgrids when it necessary. In case 2, the only actual cases of wind power data will be used since there is no effect of forecasting error on the main power fluctuation.

5.2.2.2 Case 2.

Case 2-1: 3MW –wind turbine is considered in this case. SCUC model in this case is the same as SCUC model in previous cases except for the addition of new fluctuation control constraint. This constraint is tested for various values of fluctuation limit that control dropped or increased power between two consecutive hours.

Table 5-13: The total cost for each forced limit when 3MW-wind turbine integrated with the microgrid

Fluctuation limit (MW/h)	Total Cost (($)	Lost Revenue ($)
10 (Base case)	7267.204	0.000
9	7267.204	0.000
8	7306.840	39.636
7	7320.793	53.589
6	7338.527	71.323
5	7390.831	123.627
4	7451.221	184.017
3	7534.711	267.507
2	7663.024	395.820
1	8042.171	774.967

Table 5-13 reveals the changing in the total cost for each limit. It is clear that when the limit is dropped, the total operating cost is increased. Therefore, the microgrid will be more expensive because of lost revenue. With that consideration, utilities

should take the microgrids' lost revenue into account and attempt to avoid this fluctuation in their networks.

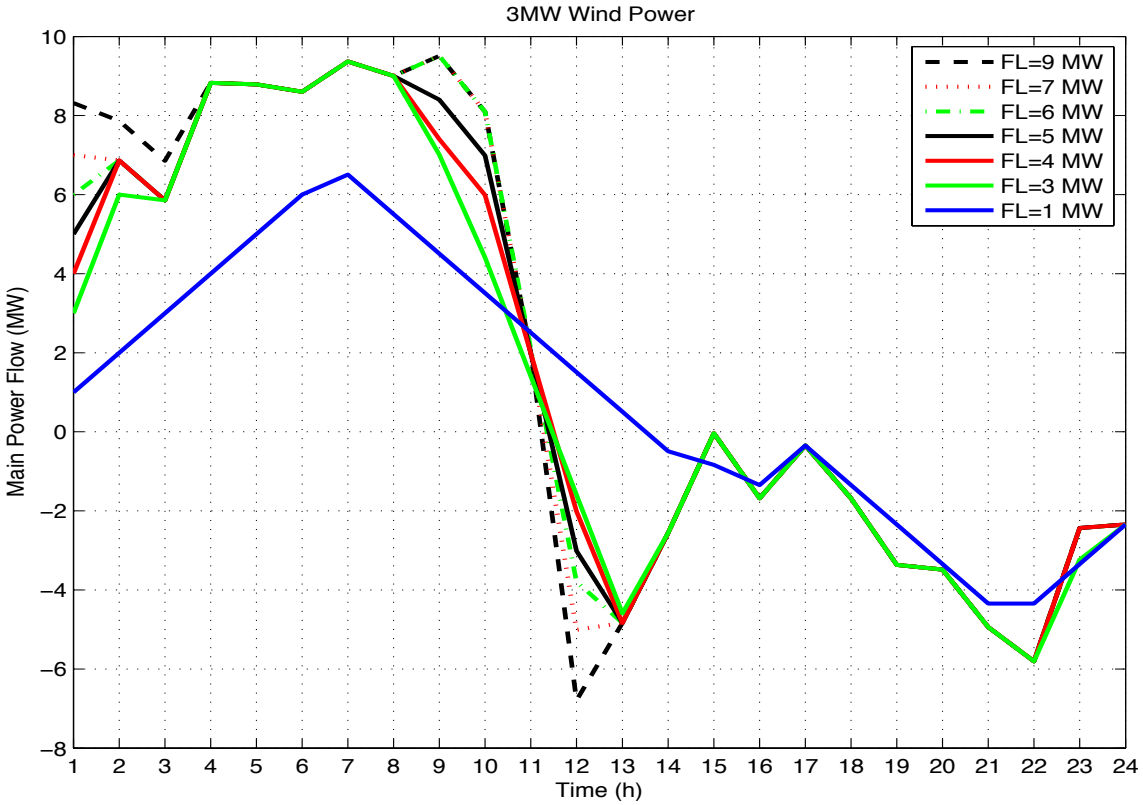

Figure 5-13: The main power flow for each fluctuation limit – 3MW-wind turbine

Figure 5-13 presents a chart for main grid power flow for each limit. The main power fluctuation is enhanced (less fluctuation) when the limit is reduced, but the total operating cost is increased.

Case 2-2: The difference in this case is wind penetration is increased to 4MW. The result is the same as the previous case. The total cost increased when the fluctuation limit reduced, but the overall total cost is less than the previous case, Table 5-14. Likewise case 2-1, Figure 5-14 shows the main power flow fluctuation is enhanced when the fluctuation limit is reduced, but it causes the microgrid more lost revenue.

Thus, it is better to increase the wind integration in the microgrids but it is worse when there is a low fluctuation limit. As a result, the microgrids operators and the utilities must compromise to decide the feasible fluctuation limit for the benefit of both.

Table 5-14: The total cost for each forced limit when 4MW-wind turbine integrated with the microgrid

Fluctuation limit (MW/h)	Total Cost ($)	Lost Revenue ($)
10 (Base case)	6433.014	0.000
9	6433.014	0.000
8	6473.021	40.007
7	6486.754	53.740
6	6509.343	76.329
5	6559.714	126.700
4	6620.880	187.866
3	6711.806	278.792
2	6861.080	428.066
1	7296.298	863.284

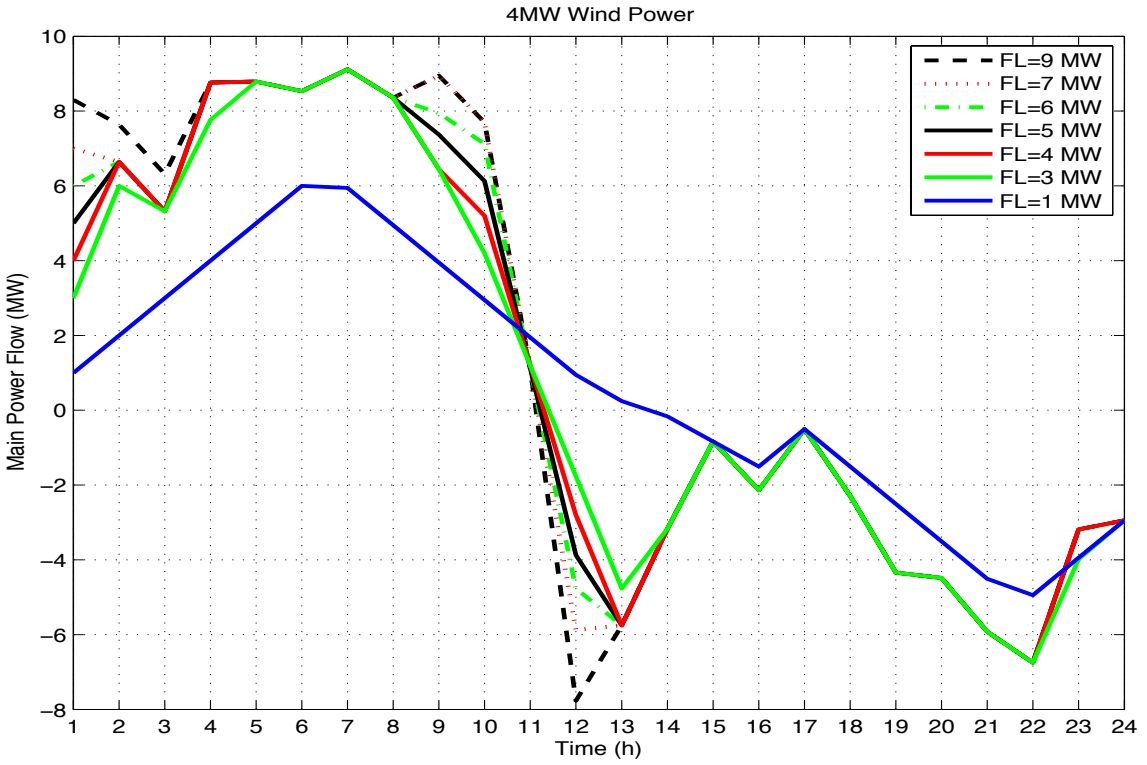

Figure 5-14: The main power flow for each fluctuation limit – 4MW-wind turbine

Table 5-15: The total cost for each forced limit when 5MW-wind turbine integrated with the microgrid

Fluctuation limit (MW/h)	Total Cost ($)	Lost Revenue ($)
10 (Base case)	5598.785	0.000
9	5598.797	0.012
8	5639.163	40.378
7	5653.210	54.425
6	5675.453	76.668
5	5729.123	130.338
4	5794.492	195.707
3	5878.871	280.086
2	6082.011	483.226
1	6568.834	970.049

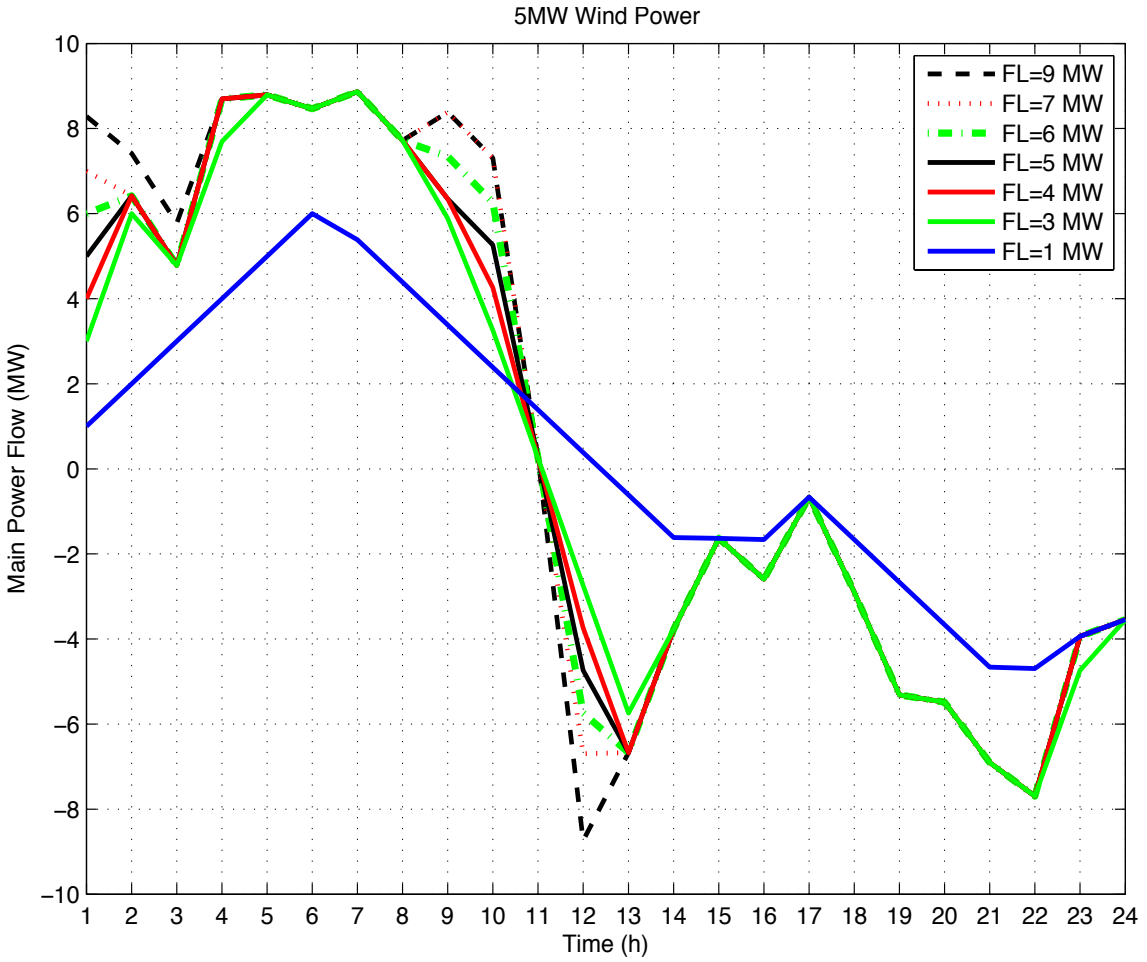

Figure 5-15: The main power flow for each fluctuation limit – 5MW-wind turbine

Case 2-3: The wind turbine capacity is increased again to be 5MW. There is no change in the results from previous sub-cases except the overall operating cost is decreased. The result of reducing the fluctuation limit stays the same as the operating cost increases, Table 5-15. Figure 5-15 also exhibits the main power flow for different values of fluctuation limit.

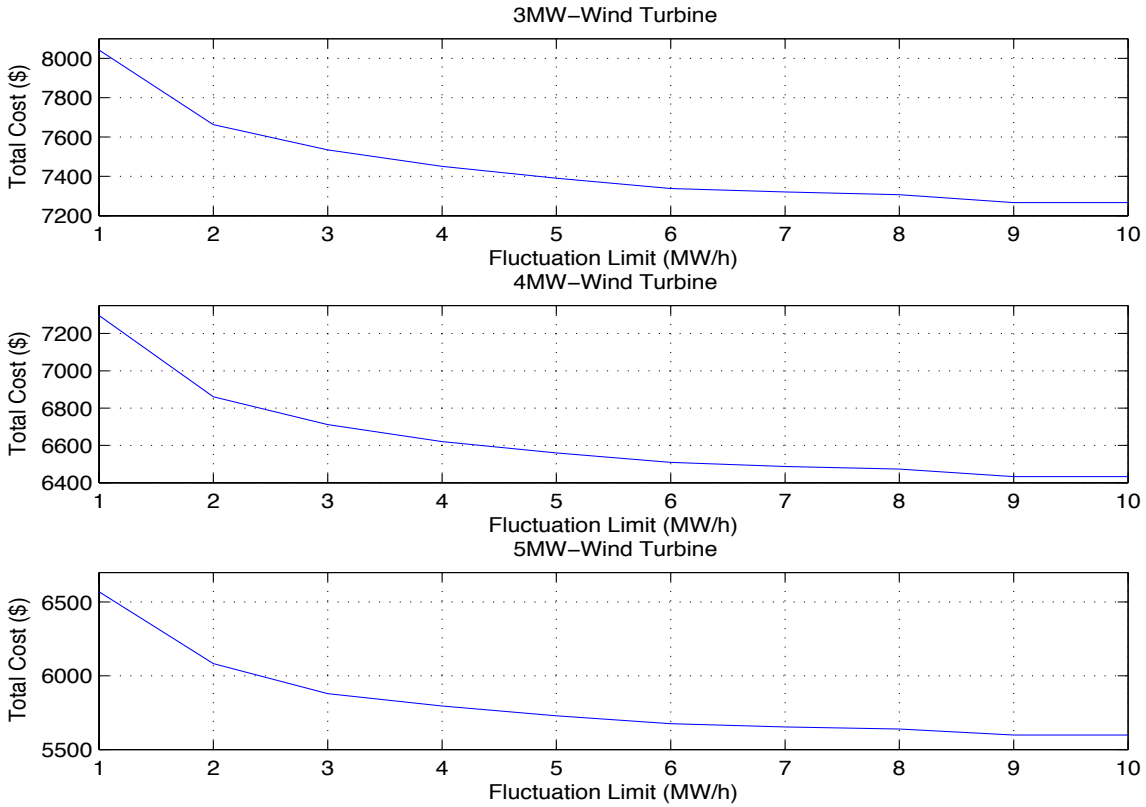

Figure 5-16: The total operating cost versus the fluctuation limits for all cases

Despite that the main power flow is enhanced when the fluctuation limit is reduced, the utility may able to meet a compromise by increasing it as the total operating cost will be high with low fluctuation limits, Figure 5-16. The total operating cost starts to rapidly increase when the fluctuation limit reduces from 5MW/h to 1MW/h and the

fluctuation of the main power flow is improved. Although the total operating cost does not increase dramatically when the fluctuation limit reduces from 10MW/h and 5MW/h, the fluctuation on the main power flow is still worse (more fluctuation) for these fluctuation limits. Figure 5-17 shows the lost revenue for each fluctuation limit for all cases.

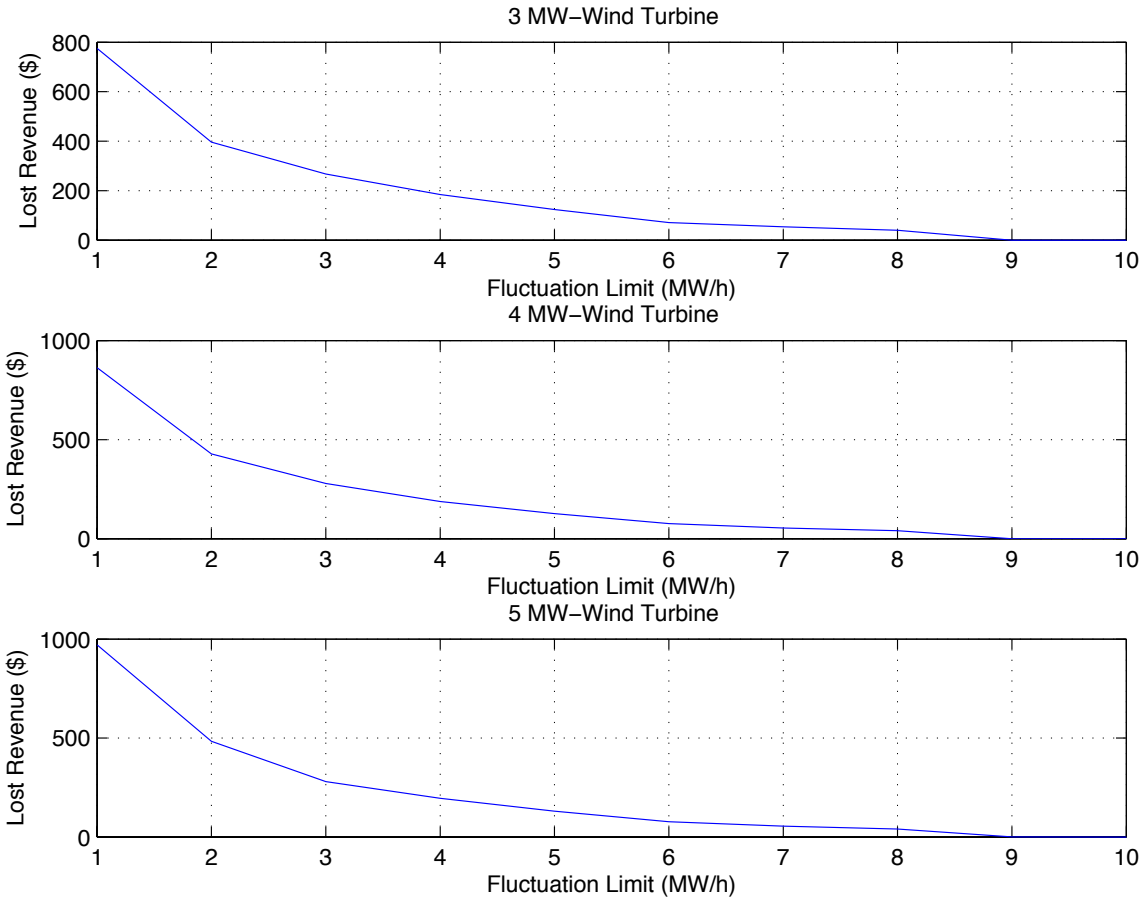

Figure 5-17: The lost revenue versus the fluctuation limits for all cases

6 Chapter Six: Conclusion and Future Work

6.1 Conclusion

This thesis relates to microgrids and the economic challenges of integrating wind energy into microgrids. Obtaining an accurate wind power forecast provides a positive impact on solving SCUC. The economic challenges include solving SCUC to achieve an optimal solution of unit scheduling and avoiding the harmful fluctuation of the main power flow.

For the purpose of wind forecasting, two forecasting models (ANN and ARIMA) were used to fit the historical wind power data. The wind power data was collected for a location near the Rocky Mountains. This data was in ten-minute step time series across a twenty-four hour period. The same data was entered as input for both models for result comparison. The comparison demonstrated that the ANN model outperformed the ARIMA model by improving the MAPE from 11.75% with ARIMA to approximately 4.60% with ANN model. This was considered to be a large improvement by reducing the MAPE nearly 60%.

A deterministic method was employed to model SCUC for the microgrid with the MILP modeling. The modeling constraints were explained in chapter four in detail. The model considered only the grid-connected mode. The dispatchable capacity of the microgrid was 16 MW. The SCUC model was validated through numerical analysis

for three cases. In the first case, the SCUC was solved for the microgrid with 3MW wind power penetration (actual date and forecasted). This demonstrated that the ANN model output provided more accurate total operating cost than ARIMA model. The same model was tested with increased wind penetration to 4MW and 5MW, second and third case respectively, with the same results. The ANN model outperformed the ARIMA model because the forecasting error (MAPE) in ANN model was much smaller than it in ARIMA. However, it was observed that the total operating cost dropped when the penetration of the wind was increased due to the wind energy being obtained at no financial charge.

Due to changing in the market prices and the cost coefficient of the microgrid's units, the main grid may experience high fluctuation in main power flow which could damage the main grid power system. Therefore, a new constraint was proposed to reduce the power flow fluctuation. This constraint employed as control the dropped or increased limit of power across two hours following. The new constraint was forced by the utility authorities on all microgrids. The SCUC was modified to add the new proposed constraint. The modified SCUC model was evaluated for the microgrid with 3MW wind power penetration (actual wind data only). The model was also appraised for different fluctuation limits ranging from 1 MW/h to 10 MW/h. The fluctuation was lower when the fluctuation limit was small and got worse when it was increased. The less fluctuation of the main power flow occurred when the fluctuation limit was reduced. Conversely, the total operating cost increased when the fluctuation limit was reduced. Consequently, the main grid operators and the microgrids operators must decide the appropriate

fluctuation limit for them at the same time. For example, they must choose a limit that enhances the harmful fluctuation without simultaneously creating a large increase in the total operating cost. The constraint was tested on higher wind penetration of 4MW and 5MW. The results did not alter, but the overall total cost decreased with increased wind penetration. As exhibited in previous figures, the power flow fluctuation was enhanced whenever fluctuation limit was reduced while the total operating cost increased sharply when fluctuation limit was reduced to be 5 MW/h and less.

In summary, the best forecasting model for short term forecasting was ANN model since it provided more accurate forecast data. The Mixed Integer Linear Programming (MILP) method became fast and provided an optimal solution for unit commitment in power system.

6.2 Future Work

This thesis can be extended to improve and get better results. There is no 100% accurate forecasting model. Researchers continue working on developing a model that gives accurate result for any data. New methods are being proposed from time to time. The forecasting models in this thesis can be developed to achieve more accurate wind power production. Moreover, hybrid model can be used to obtain more satisfied wind power forecast. ANN and ARIMA model could be combined to form a new hybrid-forecasting model.

This thesis focused on wind power deployment in microgrids. Other renewable energies can be added to this thesis such as solar power. In addition, the energy storage

system (ESS) also can be used to store unused energy and use it at peak times. By adding solar power and ESS, the microgrids become a more economic choice as these technologies also help to reduce the operating cost of the microgrids.

In addition, it is possible to extend the SCUC model, such as adding some other novel constraints to assist in obtaining the optimal solution for microgrids unit commitment. There are also other new developed unit commitment methods as descried on Table 3-1. The method that is used in this thesis is a deterministic method (MILP) which can be changed by other types of methods, such as stochastic methods, and comparing with the thesis method. Moreover, Adding cost-benefit analysis form the utilities perspective can be considered in order to find the suitable fluctuation limit considering the fluctuation limit impact on the total operating cost. Also, the work of this thesis can be extended in order to solve SCUC for high penetration of integrated microgrid in the main grid. This thesis considered only one microgrid integration, so the impact of increasing the number of integrated microgrid can be studied.

7 References

[1] "Microgrid Workshop Report August 2011.pdf." [Online]. Available: http://energy.gov/sites/prod/files/Microgrid%20Workshop%20Report%20August%202011.pdf. [Accessed: 22-Jan-2015].

[2] R. H. Lasseter, "Microgrids," in *Power Engineering Society Winter Meeting, 2002. IEEE*, 2002, vol. 1, pp. 305–308.

[3] R. H. Lasseter and P. Paigi, "Microgrid: a conceptual solution," in *Power Electronics Specialists Conference, 2004. PESC 04. 2004 IEEE 35th Annual*, 2004, vol. 6, pp. 4285–4290.

[4] A. Banerji, D. Sen, A. K. Bera, D. Ray, D. Paul, A. Bhakat, and S. K. Biswas, "Microgrid: A review," in *Global Humanitarian Technology Conference: South Asia Satellite (GHTC-SAS), 2013 IEEE*, 2013, pp. 27–35.

[5] A. Khodaei and M. Shahidehpour, "Microgrid-Based Co-Optimization of Generation and Transmission Planning in Power Systems," *IEEE Trans. Power Syst.*, vol. 28, no. 2, pp. 1582–1590, May 2013.

[6] "Microgrid Projects | Galvin Electricity Initiative." [Online]. Available: http://galvinpower.org/resources/microgrid-hub/microgrid-projects. [Accessed: 04-Sep-2014].

[7] "U.S. Mayor Article | Ansonia (CT) to Implement Energy Improvement District (July 30, 2007)." [Online]. Available: http://www.usmayors.org/usmayornewspaper/documents/07_30_07/pg8_Ansonia.asp. [Accessed: 10-Sep-2014].

[8] "A Microgrid Worth 'Bragging' About - Power Engineering."[Online]. Available: http://www.power-eng.com/articles/print/volume-107/issue-5/dg-update/a-microgrid-worth-bragging-about.html. [Accessed: 10-Sep-2014].

[9] "Local microgrid starts on $27 million | LAMonitor.com." [Online]. Available: http://www.lamonitor.com/content/local-microgrid-starts-27-million. [Accessed: 10-Sep-2014].

[10] "Smart Grid: Marin County Microgrid Project Kicks Off." [Online]. Available: http://www.smartgridnews.com/artman/publish/Delivery_Microgrids_News/Marin-County-Microgrid-Demonstration-Kicks-Off-1346.html. [Accessed: 10-Sep-2014].

[11] "Microgrid at Illinois Institute of Technology." [Online]. Available: http://www.iitmicrogrid.net/microgrid.aspx. [Accessed: 11-Sep-2014].

[12] "Galvin Conducts Naperville Smart Grid Initiative Case Study | Galvin Electricity Initiative." [Online]. Available: http://galvinpower.org/transforming-grid/perfect-power-systems/illinois/naperville. [Accessed: 11-Sep-2014].

[13] "Introduction to Perfect Power at Mesa del Sol | Galvin Electricity Initiative." [Online]. Available: http://www.galvinpower.org/transforming-grid/perfect-power-systems/prototypes/perfect-power-mesa-del-sol/introduction. [Accessed: 11-Sep-2014].

[14] "Smart Grid Today: UC San Diego gears up for 'smart microgrid'." [Online]. Available: http://www.poweranalytics.com/pa_articles/pdf/ucsd_smart_grid.pdf. [Accessed: 10-Sep-2014].

[15] T. E. Del Carpio Huayllas, D. S. Ramos, and R. L. Vasquez-Arnez, "Microgrid systems: current status and challenges," in *Transmission and Distribution Conference and Exposition: Latin America (T&D-LA), 2010 IEEE/PES*, 2010, pp. 7–12.
[16] A. A. Salam, A. Mohamed, and M. A. Hannan, "Technical challenges on microgrids," *ARPN J. Eng. Appl. Sci.*, vol. 3, no. 6, pp. 64–69, 2008.
[17] A. Khodaei, "Microgrid Optimal Scheduling With Multi-Period Islanding Constraints," *IEEE Trans. Power Syst.*, vol. 29, no. 3, pp. 1383–1392, May 2014.
[18] "Renewable Energy/MCS - Total Electrical Training." [Online]. Available: http://www.totalelectricaltraining.com/renewable-energymcs. [Accessed: 03-Dec-2014].
[19] "Eastern Rotors Group | Wind Power and More." [Online]. Available: http://easternrotors.com/en/. [Accessed: 03-Dec-2014].
[20] M. Lei, L. Shiyan, J. Chuanwen, L. Hongling, and Z. Yan, "A review on the forecasting of wind speed and generated power," *Renew. Sustain. Energy Rev.*, vol. 13, no. 4, pp. 915–920, May 2009.
[21] H. Liu, H.-Q. Tian, C. Chen, and Y. Li, "A hybrid statistical method to predict wind speed and wind power," *Renew. Energy*, vol. 35, no. 8, pp. 1857–1861, Aug. 2010.
[22] X. Wang, P. Guo, and X. Huang, "A Review of Wind Power Forecasting Models," *Energy Procedia*, vol. 12, pp. 770–778, Jan. 2011.
[23] W. Zhang, J. Wu, J. Wang, W. Zhao, and L. Shen, "Performance analysis of four modified approaches for wind speed forecasting," *Appl. Energy*, vol. 99, pp. 324–333, Nov. 2012.
[24] S. S. Soman, H. Zareipour, O. Malik, and P. Mandal, "A review of wind power and wind speed forecasting methods with different time horizons," in *North American Power Symposium (NAPS), 2010*, 2010, pp. 1–8.
[25] "[resources] SUMMARY [Week Three] - aiqus." [Online]. Available: http://www.aiqus.com/questions/7398/resources-summary-week-three. [Accessed: 03-Dec-2014].
[26] M. C. Alexiadis, P. S. Dokopoulos, and H. S. Sahsamanoglou, "Wind speed and power forecasting based on spatial correlation models," *Energy Convers. IEEE Trans. On*, vol. 14, no. 3, pp. 836–842, 1999.
[27] A. M. Foley, P. G. Leahy, A. Marvuglia, and E. J. McKeogh, "Current methods and advances in forecasting of wind power generation," *Renew. Energy*, vol. 37, no. 1, pp. 1–8, Jan. 2012.
[28] A. Togelou, G. Sideratos, and N. D. Hatziargyriou, "Wind Power Forecasting in the Absence of Historical Data," *IEEE Trans. Sustain. Energy*, vol. 3, no. 3, pp. 416–421, Jul. 2012.
[29] L. Landberg, "Short-term prediction of the power production from wind farms," *J. Wind Eng. Ind. Aerodyn.*, vol. 80, no. 1, pp. 207–220, 1999.
[30] F. Cassola and M. Burlando, "Wind speed and wind energy forecast through Kalman filtering of Numerical Weather Prediction model output," *Appl. Energy*, vol. 99, pp. 154–166, Nov. 2012.
[31] E. Erdem and J. Shi, "ARMA based approaches for forecasting the tuple of wind

speed and direction," *Appl. Energy*, vol. 88, no. 4, pp. 1405–1414, Apr. 2011.
[32] E. Cadenas and W. Rivera, "Wind speed forecasting in three different regions of Mexico, using a hybrid ARIMA–ANN model," *Renew. Energy*, vol. 35, no. 12, pp. 2732–2738, Dec. 2010.
[33] "FERC: Electric Power Markets - National Overview." [Online]. Available: http://www.ferc.gov/market-oversight/mkt-electric/overview.asp. [Accessed: 14-Oct-2014].
[34] E. Litvinov, F. Zhao, and T. Zheng, "Alternative auction objectives and pricing schemes in short-term electricity markets," in *Power & Energy Society General Meeting, 2009. PES'09. IEEE*, 2009, pp. 1–11.
[35] Mohammad Shahidehpour, Hatim Yamin, and Zuyi Li, *Market Operations in Electric Power Systems: Forecasting, Scheduling, and Risk Management*. Wiley-IEEE Press, 2002.
[36] A. Bhardwaj, V. K. Kamboj, V. K. Shukla, B. Singh, and P. Khurana, "Unit commitment in electrical power system-a literature review," in *Power Engineering and Optimization Conference (PEDCO) Melaka, Malaysia, 2012 Ieee International*, 2012, pp. 275–280.
[37] B. Wright, "A Review of Unit Commitment," 2013.
[38] T. Logenthiran and D. Srinivasan, "Formulation of unit commitment (UC) problems and analysis of available methodologies used for solving the problems," in *Sustainable Energy Technologies (ICSET), 2010 IEEE International Conference on*, 2010, pp. 1–6.
[39] P. Goodwin and R. Lawton, "On the asymmetry of the symmetric MAPE," *Int. J. Forecast.*, vol. 15, no. 4, pp. 405–408, Oct. 1999.
[40] "NREL: Western Wind Resources Dataset." [Online]. Available: http://wind.nrel.gov/Web_nrel/. [Accessed: 10-Dec-2014].